US012386030B2

(12) **United States Patent**
Ali et al.

(10) **Patent No.: US 12,386,030 B2**
(45) **Date of Patent: *Aug. 12, 2025**

(54) **METHOD AND SYSTEM FOR ANTENNA ARRAY CALIBRATION FOR CROSS-COUPLING AND GAIN/PHASE VARIATIONS IN RADAR SYSTEMS**

(71) Applicant: **UHNDER, INC.**, Austin, TX (US)

(72) Inventors: **Murtaza Ali**, Cedar Park, TX (US); **Ali Erdem Ertan**, Austin, TX (US); **Kevin B. Foltinek**, Austin, TX (US)

(73) Assignee: **Robert Bosch GMBH**, Gerlingen (DE)

(*) Notice: Subject to any disclaimer, the term of this patent is extended or adjusted under 35 U.S.C. 154(b) by 0 days.

This patent is subject to a terminal disclaimer.

(21) Appl. No.: **18/630,364**

(22) Filed: **Apr. 9, 2024**

(65) **Prior Publication Data**

US 2024/0272276 A1 Aug. 15, 2024

Related U.S. Application Data

(63) Continuation of application No. 17/147,914, filed on Jan. 13, 2021, now Pat. No. 11,953,615.
(Continued)

(51) **Int. Cl.**
G01S 7/35 (2006.01)
G01S 7/02 (2006.01)
(Continued)

(52) **U.S. Cl.**
CPC ***G01S 7/352*** (2013.01); ***G01S 7/023*** (2013.01); ***G01S 7/4004*** (2013.01); ***G01S 13/34*** (2013.01);
(Continued)

(58) **Field of Classification Search**
CPC G01S 7/352; G01S 7/023; G01S 7/4004; G01S 13/34; G01S 13/584; G01S 13/588;
(Continued)

(56) **References Cited**

U.S. PATENT DOCUMENTS

1,882,128 A 10/1932 Fearing
3,374,478 A 3/1968 Blau
(Continued)

FOREIGN PATENT DOCUMENTS

EP 0509843 10/1992
EP 1826586 8/2007
(Continued)

OTHER PUBLICATIONS

Chambers et al., "An article entitled Real-Time Vehicle Mounted Multistatic Ground Penetrating Radar Imaging System for Buried Object Detection," Lawrence Livermore National Laboratory Reports (LLNL-TR-615452), Feb. 4, 2013; Retrieved from the Internet from https://e-reports-ext.llnl.gov/pdf/711892.pdf.
(Continued)

Primary Examiner — William Kelleher
Assistant Examiner — Ismaaeel A. Siddiquee
(74) *Attorney, Agent, or Firm* — Gardner, Linn, Burkhart & Ondersma LLP

(57) **ABSTRACT**

A radar system with on-system calibration includes capabilities for radar detection and correction for system impairments to improve detection performance. The radar system is equipped with pluralities of transmit antennas and pluralities of receive antennas. The radar system uses a series of calibration measurements of a known object to estimate the system impairments. A correction is then applied to the beamforming weights to mitigate the effect of these impairments on radar detection. The estimation and correction requires no external measurement equipment and can be computed on the radar system itself.

26 Claims, 10 Drawing Sheets

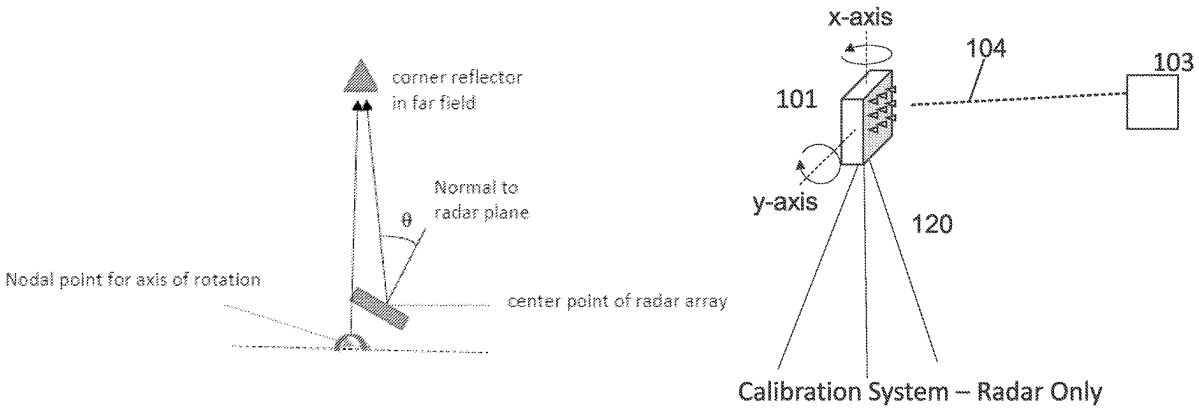

Related U.S. Application Data

(60) Provisional application No. 62/960,220, filed on Jan. 13, 2020.

(51) **Int. Cl.**

G01S 7/28	(2006.01)
G01S 7/32	(2006.01)
G01S 7/40	(2006.01)
G01S 13/34	(2006.01)
G01S 13/36	(2006.01)
G01S 13/42	(2006.01)
G01S 13/58	(2006.01)
G01S 13/87	(2006.01)
G01S 13/931	(2020.01)
H01Q 3/26	(2006.01)

(52) **U.S. Cl.**

CPC ***G01S 13/584*** (2013.01); ***G01S 13/588*** (2013.01); ***G01S 13/931*** (2013.01); ***H01Q 3/267*** (2013.01); *G01S 7/28* (2013.01); *G01S 7/32* (2013.01); *G01S 7/356* (2021.05); *G01S 13/36* (2013.01); *G01S 13/42* (2013.01); *G01S 13/878* (2013.01); *G01S 2013/93271* (2020.01); *G01S 2013/93272* (2020.01)

(58) **Field of Classification Search**

CPC . G01S 13/931; G01S 7/28; G01S 7/32; G01S 7/356; G01S 13/36; G01S 13/42; G01S 13/878; G01S 2013/93271; G01S 2013/93272; G01S 7/032; G01S 7/028; H01Q 3/267

See application file for complete search history.

(56) **References Cited**

U.S. PATENT DOCUMENTS

3,735,398	A		5/1973	Ross
3,750,169	A		7/1973	Strenglein
3,766,554	A		10/1973	Tresselt
3,896,434	A		7/1975	Sirven
3,932,871	A		1/1976	Foote
4,078,234	A		3/1978	Fishbein et al.
4,176,351	A		11/1979	De Vita et al.
4,308,536	A		12/1981	Sims, Jr. et al.
4,566,010	A		1/1986	Collins
4,612,547	A		9/1986	Itoh
4,882,668	A		11/1989	Schmid et al.
4,910,464	A		3/1990	Trett et al.
4,939,685	A		7/1990	Feintuch
5,001,486	A		3/1991	Bächtiger
5,012,254	A		4/1991	Thompson
5,034,906	A		7/1991	Chang
5,087,918	A		2/1992	May et al.
5,140,331	A	*	8/1992	Aulenbacher G01S 7/4004 342/192
5,170,331	A		8/1992	Aulenbacher et al.
5,151,702	A		9/1992	Urkowitz
5,175,710	A		12/1992	Hutson
5,218,619	A		6/1993	Dent
5,272,663	A		12/1993	Jones et al.
5,280,288	A		1/1994	Sherry et al.
5,302,956	A		4/1994	Asbury et al.
5,341,141	A		8/1994	Frazier et al.
5,345,470	A		9/1994	Alexander
5,361,072	A		11/1994	Barrick et al.
5,376,939	A		12/1994	Urkowitz
5,379,322	A		1/1995	Kosaka et al.
5,436,872	A		7/1995	Gilmour et al.
5,497,162	A		3/1996	Kaiser
5,508,706	A		4/1996	Tsou et al.
5,581,464	A		12/1996	Woll et al.
5,654,715	A		8/1997	Hayashikura et al.
5,657,021	A		8/1997	Ehsani-Nategh et al.
5,657,023	A		8/1997	Lewis et al.
5,682,605	A		10/1997	Salter
5,691,724	A		11/1997	Aker et al.
5,712,640	A		1/1998	Andou
5,724,041	A		3/1998	Inoue et al.
5,847,661	A		12/1998	Ricci
5,861,834	A		1/1999	Sauer et al.
5,892,477	A		4/1999	Wehling
5,917,430	A		6/1999	Greneker, III et al.
5,920,278	A		7/1999	Tyler et al.
5,920,285	A		7/1999	Benjamin
5,931,893	A		8/1999	Dent et al.
5,959,571	A		9/1999	Aoyagi et al.
5,970,400	A		10/1999	Dwyer
6,048,315	A		4/2000	Chiao et al.
6,067,314	A		5/2000	Azuma
6,069,581	A		5/2000	Bell et al.
6,121,872	A		9/2000	Weishaupt
6,121,918	A		9/2000	Tullsson
6,151,366	A		11/2000	Yip
6,163,252	A		12/2000	Nishiwaki
6,184,829	B1		2/2001	Stilp
6,191,726	B1		2/2001	Tullsson
6,208,248	B1		3/2001	Ross
6,288,672	B1		9/2001	Asano et al.
6,307,622	B1		10/2001	Lewis
6,335,700	B1		1/2002	Ashihara
6,347,264	B2		2/2002	Nicosia et al.
6,396,436	B1		5/2002	Lissel et al.
6,400,308	B1		6/2002	Bell et al.
6,411,250	B1		6/2002	Oswald et al.
6,417,796	B1		7/2002	Bowlds
6,424,289	B2		7/2002	Fukae et al.
6,529,931	B1		3/2003	Besz et al.
6,547,733	B2		4/2003	Hwang et al.
6,583,753	B1		6/2003	Reed
6,614,387	B1		9/2003	Deadman
6,624,784	B1		9/2003	Yamaguchi
6,674,908	B1		1/2004	Aronov
6,683,560	B2		1/2004	Bauhahn
6,693,582	B2		2/2004	Steinlechner et al.
6,714,956	B1		3/2004	Liu et al.
6,747,595	B2		6/2004	Hirabe
6,768,391	B1		7/2004	Dent et al.
6,865,218	B1		3/2005	Sourour
6,867,732	B1		3/2005	Chen et al.
6,888,491	B2		5/2005	Richter
6,975,246	B1		12/2005	Trudeau
7,066,886	B2		6/2006	Song et al.
7,119,739	B1		10/2006	Struckman
7,130,663	B2		10/2006	Guo
7,202,776	B2		4/2007	Breed
7,289,058	B2		10/2007	Shima
7,299,251	B2		11/2007	Skidmore et al.
7,338,450	B2		3/2008	Kristofferson et al.
7,395,084	B2		7/2008	Anttila
7,460,055	B2		12/2008	Nishijima et al.
7,474,258	B1		1/2009	Arikan et al.
7,545,310	B2		6/2009	Matsuoka
7,545,321	B2		6/2009	Kawasaki
7,564,400	B2		7/2009	Fukuda
7,567,204	B2		7/2009	Sakamoto
7,609,198	B2		10/2009	Chang
7,642,952	B2		1/2010	Fukuda
7,663,533	B2		2/2010	Toennesen
7,667,637	B2		2/2010	Pedersen et al.
7,728,762	B2		6/2010	Sakamoto
7,791,528	B2		9/2010	Klotzbuecher
7,847,731	B2		12/2010	Wiesbeck et al.
7,855,677	B2		12/2010	Negoro et al.
7,859,450	B2		12/2010	Shirakawa et al.
8,019,352	B2		9/2011	Rappaport et al.
8,044,845	B2		10/2011	Saunders
8,049,663	B2		11/2011	Frank et al.
8,059,026	B1		11/2011	Nunez
8,102,306	B2		1/2012	Smith, Jr. et al.
8,115,672	B2		2/2012	Nouvel et al.
8,154,436	B2		4/2012	Szajnowski
8,169,359	B2		5/2012	Aoyagi

(56) **References Cited**

U.S. PATENT DOCUMENTS

8,212,713 B2 7/2012 Aiga et al.
8,330,650 B2 12/2012 Goldman
8,390,507 B2 3/2013 Wintermantel
8,471,760 B2 6/2013 Szajnowski
8,532,159 B2 9/2013 Kagawa et al.
8,547,988 B2 10/2013 Hadani et al.
8,686,894 B2 4/2014 Fukuda et al.
8,694,306 B1 4/2014 Short et al.
8,768,248 B2 7/2014 Sadr
8,994,581 B1 3/2015 Brown
9,020,011 B1 4/2015 Hiebert et al.
9,063,225 B2 6/2015 Lee et al.
9,121,943 B2 9/2015 Stirlin-Gallacher et al.
9,182,479 B2 11/2015 Chen et al.
9,194,946 B1 11/2015 Vacanti
9,239,378 B2 1/2016 Kishigami et al.
9,239,379 B2 1/2016 Burgio et al.
9,274,217 B2 3/2016 Chang et al.
9,282,945 B2 3/2016 Smith et al.
9,335,402 B2 5/2016 Maeno et al.
9,400,328 B2 7/2016 Hsiao et al.
9,541,639 B2 1/2017 Searcy et al.
9,568,600 B2 2/2017 Alland
9,575,160 B1 2/2017 Davis et al.
9,599,702 B1 3/2017 Bordes et al.
9,618,616 B2 4/2017 Kishigami et al.
9,689,967 B1 6/2017 Stark et al.
9,709,674 B2 7/2017 Moriuchi et al.
9,720,073 B1 8/2017 Davis et al.
9,726,756 B2 8/2017 Jansen
9,720,080 B1 9/2017 Rodenbeck
9,753,121 B1 9/2017 Davis
9,753,132 B1 9/2017 Bordes et al.
9,772,397 B1 9/2017 Bordes et al.
9,791,551 B1 10/2017 Eshraghi et al.
9,791,564 B1 10/2017 Harris et al.
9,806,914 B1 10/2017 Bordes et al.
9,829,567 B1 11/2017 Davis et al.
9,846,228 B2 12/2017 Davis et al.
9,869,762 B1 1/2018 Alland et al.
9,945,935 B2 4/2018 Eshraghi et al.
9,954,955 B2 4/2018 Davis et al.
9,971,020 B1 5/2018 Maher et al.
9,989,627 B2 6/2018 Eshraghi et al.
9,989,638 B2 6/2018 Harris et al.
10,073,171 B2 9/2018 Bordes et al.
10,090,585 B2 10/2018 Dinc et al.
10,092,192 B2 10/2018 Lashkari et al.
10,142,133 B2 11/2018 Bordes et al.
10,145,954 B2 12/2018 Davis et al.
10,191,142 B2 1/2019 Eshraghi et al.
10,197,671 B2 2/2019 Alland et al.
10,215,853 B2 2/2019 Stark et al.
10,261,179 B2 4/2019 Davis et al.
10,305,611 B1 5/2019 Rimini et al.
10,324,165 B2 6/2019 Bordes et al.
10,371,797 B1 8/2019 Prados et al.
10,386,470 B2 8/2019 Zivkovic
10,536,529 B2 1/2020 Davis et al.
10,551,482 B2 2/2020 Eshraghi et al.
10,573,959 B2 2/2020 Alland et al.
10,594,916 B2 3/2020 Sivan
10,605,894 B2 3/2020 Davis et al.
10,659,078 B2 5/2020 Nayyar et al.
10,670,695 B2 6/2020 Maher et al.
10,690,780 B1 * 6/2020 Zarubica G01S 19/32
10,775,478 B2 9/2020 Davis et al.
10,782,389 B2 9/2020 Rao et al.
10,805,933 B2 10/2020 Stephens et al.
10,812,985 B2 10/2020 Mody et al.
10,852,408 B2 12/2020 Aslett et al.
10,866,306 B2 12/2020 Maher et al.
10,908,272 B2 2/2021 Rao et al.
10,935,633 B2 3/2021 Maher et al.
10,976,431 B2 4/2021 Harris et al.
11,054,516 B2 7/2021 Wu et al.
11,086,010 B2 8/2021 Davis et al.
11,105,890 B2 8/2021 Behrens et al.
11,175,377 B2 11/2021 Bordes et al.
11,194,016 B2 12/2021 Eshraghi et al.
11,262,448 B2 3/2022 Davis et al.
11,271,328 B2 3/2022 Liu et al.
11,340,331 B2 5/2022 Maher et al.
11,454,697 B2 9/2022 Maher et al.
11,474,225 B2 10/2022 Dent et al.
11,582,305 B2 2/2023 Davis et al.
11,681,017 B2 6/2023 Behrens et al.
11,726,172 B2 8/2023 Maher et al.
11,740,323 B2 8/2023 Davis et al.
11,846,696 B2 12/2023 Rao et al.
2001/0002919 A1 6/2001 Sourour et al.
2002/0004692 A1 1/2002 Nicosia et al.
2002/0044082 A1 4/2002 Woodington et al.
2002/0063653 A1 5/2002 Oey et al.
2002/0075178 A1 6/2002 Woodington et al.
2002/0118522 A1 8/2002 Ho et al.
2002/0130811 A1 9/2002 Voigtlaender
2002/0147534 A1 10/2002 Delcheccolo et al.
2002/0155811 A1 10/2002 Prismantas
2003/0001772 A1 1/2003 Woodington et al.
2003/0011519 A1 1/2003 Breglia et al.
2003/0058166 A1 3/2003 Hirabe
2003/0073463 A1 4/2003 Shapira
2003/0080713 A1 5/2003 Kirmuss
2003/0102997 A1 6/2003 Levin et al.
2003/0164791 A1 9/2003 Shinoda et al.
2003/0228890 A1 12/2003 Falaki
2003/0235244 A1 12/2003 Pessoa et al.
2004/0012516 A1 1/2004 Schiffmann
2004/0015529 A1 1/2004 Tanrkulu et al.
2004/0066323 A1 4/2004 Richter
2004/0070532 A1 4/2004 Ishii et al.
2004/0107030 A1 6/2004 Nishira et al.
2004/0130486 A1 7/2004 Akopian
2004/0138802 A1 7/2004 Kuragaki et al.
2004/0215373 A1 10/2004 Won et al.
2004/0229590 A1 11/2004 Kubo et al.
2005/0001757 A1 1/2005 Shinoda et al.
2005/0008065 A1 1/2005 Schilling
2005/0069162 A1 3/2005 Haykin
2005/0090274 A1 4/2005 Miyashita
2005/0100106 A1 5/2005 Chen
2005/0156780 A1 7/2005 Bonthron et al.
2005/0201457 A1 9/2005 Allred et al.
2005/0225476 A1 10/2005 Hoetzel et al.
2005/0273480 A1 12/2005 Pugh et al.
2006/0012511 A1 1/2006 Dooi et al.
2006/0036353 A1 2/2006 Wintermantel
2006/0050707 A1 3/2006 Sterin
2006/0093078 A1 5/2006 Lewis et al.
2006/0109170 A1 5/2006 Voigtlaender et al.
2006/0109931 A1 5/2006 Asai
2006/0114324 A1 6/2006 Farmer et al.
2006/0140249 A1 6/2006 Kohno
2006/0181448 A1 8/2006 Natsume et al.
2006/0220943 A1 10/2006 Schlick et al.
2006/0244653 A1 11/2006 Szajnowski
2006/0262007 A1 11/2006 Bonthron
2006/0262009 A1 11/2006 Watanabe
2007/0018884 A1 1/2007 Adams
2007/0018886 A1 1/2007 Watanabe et al.
2007/0040729 A1 2/2007 Ohnishi
2007/0096885 A1 5/2007 Cheng et al.
2007/0109175 A1 5/2007 Fukuda
2007/0115869 A1 5/2007 Lakkis
2007/0120731 A1 5/2007 Kelly, Jr. et al.
2007/0132633 A1 6/2007 Uchino
2007/0152870 A1 7/2007 Woodington et al.
2007/0152871 A1 7/2007 Puglia
2007/0152872 A1 7/2007 Woodington
2007/0164896 A1 7/2007 Suzuki et al.
2007/0171122 A1 7/2007 Nakano
2007/0182619 A1 8/2007 Honda et al.
2007/0182623 A1 8/2007 Zeng

(56) **References Cited**

U.S. PATENT DOCUMENTS

2007/0188373 A1 8/2007 Shirakawa et al.
2007/0200747 A1 8/2007 Okai
2007/0205937 A1 9/2007 Thompson
2007/0263748 A1 11/2007 Mesecher
2007/0279303 A1 12/2007 Schoebel
2008/0012710 A1 1/2008 Sadr
2008/0080599 A1 4/2008 Kang
2008/0088499 A1 4/2008 Bonthron
2008/0094274 A1 4/2008 Nakanishi
2008/0106458 A1 5/2008 Honda et al.
2008/0150790 A1 6/2008 Voigtlaender et al.
2008/0180311 A1 7/2008 Mikami
2008/0208472 A1 8/2008 Morcom
2008/0218406 A1 9/2008 Nakanishi
2008/0258964 A1 10/2008 Schoeberl
2008/0272955 A1 11/2008 Yonak et al.
2009/0003412 A1 1/2009 Negoro et al.
2009/0015459 A1 1/2009 Mahler et al.
2009/0015464 A1 1/2009 Fukuda
2009/0021429 A1 1/2009 Colburn et al.
2009/0027257 A1 1/2009 Arikan
2009/0046000 A1 2/2009 Matsuoka
2009/0051581 A1 2/2009 Hatono
2009/0072957 A1 3/2009 Wu et al.
2009/0073025 A1 3/2009 Inoue et al.
2009/0074031 A1 3/2009 Fukuda
2009/0079617 A1 3/2009 Shirakawa et al.
2009/0085827 A1 4/2009 Orime et al.
2009/0103593 A1 4/2009 Bergamo
2009/0121918 A1 5/2009 Shirai et al.
2009/0212998 A1 8/2009 Szajnowski
2009/0232510 A1 9/2009 Gupta et al.
2009/0237293 A1 9/2009 Sakuma
2009/0254260 A1 10/2009 Nix et al.
2009/0267822 A1 10/2009 Shinoda et al.
2009/0289831 A1 11/2009 Akita
2009/0295623 A1 12/2009 Falk
2010/0001897 A1 1/2010 Lyman
2010/0019950 A1 1/2010 Yamano et al.
2010/0039311 A1 2/2010 Woodington et al.
2010/0039313 A1 2/2010 Morris
2010/0075704 A1 3/2010 McHenry et al.
2010/0116365 A1 5/2010 McCarty
2010/0127916 A1 5/2010 Sakai et al.
2010/0156690 A1 6/2010 Kim et al.
2010/0166121 A1 7/2010 Kenney, Jr.
2010/0198513 A1 8/2010 Zeng et al.
2010/0202495 A1 8/2010 Kagawa et al.
2010/0253573 A1 10/2010 Holzheimer et al.
2010/0277359 A1 11/2010 Ando
2010/0289692 A1 11/2010 Winkler
2011/0006944 A1 1/2011 Goldman
2011/0032138 A1 2/2011 Krapf
2011/0074620 A1 3/2011 Wintermantel
2011/0187600 A1 8/2011 Landt
2011/0196568 A1 8/2011 Nickolaou
2011/0234448 A1 9/2011 Hayase
2011/0248796 A1 10/2011 Pozgay
2011/0279303 A1 11/2011 Smith, Jr. et al.
2011/0279307 A1 11/2011 Song
2011/0285576 A1 11/2011 Lynam
2011/0291874 A1 12/2011 De Mersseman
2011/0291875 A1 12/2011 Szajnowski
2011/0292971 A1 12/2011 Hadani et al.
2011/0298653 A1 12/2011 Mizutani
2012/0001791 A1 1/2012 Wintermantel
2012/0050092 A1 3/2012 Lee et al.
2012/0050093 A1 3/2012 Heilmann et al.
2012/0105268 A1 5/2012 Smits et al.
2012/0112957 A1 5/2012 Nguyen et al.
2012/0133547 A1 5/2012 MacDonald et al.
2012/0146834 A1 6/2012 Karr
2012/0173246 A1 7/2012 Choi et al.
2012/0194377 A1 8/2012 Yukmatsu et al.
2012/0195349 A1 8/2012 Lakkis
2012/0235857 A1 9/2012 Kim et al.
2012/0249356 A1 10/2012 Shope
2012/0257643 A1 10/2012 Wu et al.
2012/0283987 A1 11/2012 Busking et al.
2012/0314799 A1 12/2012 In De Betou et al.
2012/0319900 A1 12/2012 Johansson et al.
2013/0016761 A1 1/2013 Nentwig
2013/0021196 A1 1/2013 Himmelstoss
2013/0027240 A1 1/2013 Chowdhury
2013/0057436 A1 3/2013 Krasner et al.
2013/0069818 A1 3/2013 Shirakawa et al.
2013/0102254 A1 4/2013 Cyzs
2013/0113647 A1 5/2013 Sentelle et al.
2013/0113652 A1 5/2013 Smits et al.
2013/0113653 A1 5/2013 Kishigami et al.
2013/0129253 A1* 5/2013 Moate G01S 13/90 382/278
2013/0135140 A1 5/2013 Kishigami
2013/0169468 A1 7/2013 Johnson et al.
2013/0169485 A1 7/2013 Lynch
2013/0176154 A1 7/2013 Bonaccio et al.
2013/0194127 A1 8/2013 Ishihara et al.
2013/0214961 A1 8/2013 Lee et al.
2013/0229301 A1 9/2013 Kanamoto
2013/0244710 A1 9/2013 Nguyen et al.
2013/0249730 A1 9/2013 Adcook
2013/0314271 A1 11/2013 Braswell et al.
2013/0321196 A1 12/2013 Binzer et al.
2014/0022108 A1 1/2014 Alberth, Jr. et al.
2014/0028491 A1 1/2014 Ferguson
2014/0035774 A1 2/2014 Khlifi
2014/0049423 A1 2/2014 De Jong et al.
2014/0070985 A1 3/2014 Vacanti
2014/0085128 A1 3/2014 Kishigami et al.
2014/0097987 A1 4/2014 Worl et al.
2014/0111367 A1 4/2014 Kishigami et al.
2014/0111372 A1 4/2014 Wu
2014/0139322 A1 5/2014 Wang et al.
2014/0159948 A1 6/2014 Ishimori et al.
2014/0168004 A1 6/2014 Chen et al.
2014/0218240 A1 8/2014 Kpodzo et al.
2014/0220903 A1 8/2014 Schulz et al.
2014/0253345 A1 9/2014 Breed
2014/0253364 A1 9/2014 Lee et al.
2014/0285373 A1 9/2014 Kuwahara et al.
2014/0316261 A1 10/2014 Lux et al.
2014/0327566 A1 11/2014 Burgio et al.
2014/0327570 A1 11/2014 Beyer
2014/0340254 A1 11/2014 Hesse
2014/0348253 A1 11/2014 Mobasher et al.
2014/0350815 A1 11/2014 Kambe
2015/0002329 A1 1/2015 Murad et al.
2015/0002357 A1 1/2015 Sanford et al.
2015/0035662 A1 2/2015 Bowers et al.
2015/0061922 A1 3/2015 Kishigami
2015/0103745 A1 4/2015 Negus et al.
2015/0153445 A1 6/2015 Jansen
2015/0160335 A1 6/2015 Lynch et al.
2015/0198709 A1 7/2015 Inoue
2015/0204966 A1 7/2015 Kishigami
2015/0204971 A1 7/2015 Yoshimura et al.
2015/0204972 A1 7/2015 Kuehnle et al.
2015/0226838 A1 8/2015 Hayakawa
2015/0226848 A1 8/2015 Park
2015/0234045 A1 8/2015 Rosenblum
2015/0247924 A1 9/2015 Kishigami
2015/0255867 A1 9/2015 Inoue
2015/0280893 A1 10/2015 Choi et al.
2015/0301172 A1 10/2015 Ossowska
2015/0323660 A1 11/2015 Hampikian
2015/0331090 A1 11/2015 Jeong et al.
2015/0333847 A1 11/2015 Bharadia et al.
2015/0346323 A1 12/2015 Kollmer
2015/0369912 A1 12/2015 Kishigami et al.
2015/0373167 A1 12/2015 Murashov et al.
2016/0003935 A1 1/2016 Stainvas Olshansky et al.
2016/0003938 A1 1/2016 Gazit et al.
2016/0003939 A1 1/2016 Stainvas Olshansky et al.
2016/0018511 A1 1/2016 Nayyar et al.

(56) **References Cited**

U.S. PATENT DOCUMENTS

2016/0025844 A1 1/2016 Mckitterick et al.
2016/0033623 A1 2/2016 Holder
2016/0033631 A1 2/2016 Searcy et al.
2016/0033632 A1 2/2016 Searcy et al.
2016/0041260 A1 2/2016 Cao et al.
2016/0054441 A1 2/2016 Kuo et al.
2016/0061935 A1 3/2016 McCloskey et al.
2016/0084941 A1 3/2016 Arage
2016/0084943 A1 3/2016 Arage
2016/0091595 A1 3/2016 Alcalde
2016/0103206 A1 4/2016 Pavao-Moreira et al.
2016/0124075 A1 5/2016 Vogt et al.
2016/0124086 A1 5/2016 Jansen et al.
2016/0131742 A1 5/2016 Schoor
2016/0131752 A1 5/2016 Jansen et al.
2016/0139254 A1 5/2016 Wittenberg
2016/0146931 A1 5/2016 Rao et al.
2016/0154103 A1 6/2016 Moriuchi
2016/0157828 A1 6/2016 Sumi et al.
2016/0178732 A1 6/2016 Oka et al.
2016/0213258 A1 7/2016 Lashkari et al.
2016/0223643 A1 8/2016 Li et al.
2016/0223644 A1 8/2016 Soga
2016/0238694 A1 8/2016 Kishigami
2016/0245909 A1 8/2016 Aslett et al.
2016/0291130 A1 10/2016 Ginsburg et al.
2016/0349365 A1 12/2016 Ling
2017/0010361 A1 1/2017 Tanaka
2017/0023661 A1 1/2017 Richert
2017/0023663 A1 1/2017 Subburaj et al.
2017/0045608 A1 2/2017 Mclean et al.
2017/0074980 A1 3/2017 Adib
2017/0090015 A1 3/2017 Breen et al.
2017/0117946 A1* 4/2017 Lee G01S 3/72
2017/0117950 A1 4/2017 Strong
2017/0153315 A1 6/2017 Katayama
2017/0153316 A1 6/2017 Wintermantel
2017/0176583 A1 6/2017 Gulden et al.
2017/0212213 A1 7/2017 Kishigami
2017/0219689 A1 8/2017 Hung et al.
2017/0223712 A1 8/2017 Stephens et al.
2017/0234968 A1 8/2017 Roger et al.
2017/0254879 A1 9/2017 Tokieda, I et al.
2017/0293027 A1 10/2017 Stark et al.
2017/0307728 A1 10/2017 Eshraghi et al.
2017/0307729 A1 10/2017 Eshraghi et al.
2017/0309997 A1 10/2017 Alland et al.
2017/0310758 A1* 10/2017 Davis G01S 13/931
2017/0363731 A1 12/2017 Bordes et al.
2018/0003799 A1 1/2018 Yang et al.
2018/0019755 A1 1/2018 Josefsberg et al.
2018/0175907 A1 1/2018 Marr
2018/0031674 A1 2/2018 Bordes et al.
2018/0031675 A1 2/2018 Eshraghi et al.
2018/0095161 A1 4/2018 Kellum et al.
2018/0095163 A1 4/2018 Lovberg et al.
2018/0113191 A1 4/2018 Villeval et al.
2018/0115371 A1 4/2018 Trotta et al.
2018/0128913 A1 5/2018 Bialer
2018/0149730 A1 5/2018 Li et al.
2018/0149736 A1 5/2018 Alland et al.
2018/0231655 A1 8/2018 Stark et al.
2018/0271776 A1 9/2018 Kazakevitch
2018/0294564 A1* 10/2018 Kim H01Q 3/2652
2018/0294908 A1 10/2018 Abdelmonem
2018/0329027 A1 11/2018 Eshraghi et al.
2018/0358706 A1 12/2018 Kildal et al.
2018/0372837 A1 12/2018 Bily et al.
2018/0374346 A1 12/2018 Fowe
2019/0013566 A1* 1/2019 Merrell H01Q 1/1257
2019/0056476 A1 2/2019 Lin
2019/0064364 A1 2/2019 Boysel et al.
2019/0072641 A1 3/2019 Al-Stouhi et al.
2019/0146059 A1 5/2019 Zanati et al.
2019/0178983 A1 6/2019 Lin et al.
2019/0187245 A1 6/2019 Guarin Aristizabal et al.
2019/0219685 A1 7/2019 Shan
2019/0235050 A1 8/2019 Maligeorgos et al.
2019/0293755 A1 9/2019 Cohen et al.
2019/0324134 A1 10/2019 Cattle
2019/0377077 A1 12/2019 Kitayama et al.
2019/0379386 A1 12/2019 Chi
2019/0383929 A1 12/2019 Melzer et al.
2020/0003884 A1 1/2020 Arkind et al.
2020/0011983 A1 1/2020 Kageme et al.
2020/0014105 A1* 1/2020 Braun H01Q 3/267
2020/0033445 A1* 1/2020 Raphaeli H01Q 1/38
2020/0036487 A1 1/2020 Hammond et al.
2020/0064455 A1 2/2020 Schroder et al.
2020/0107249 A1 4/2020 Stauffer et al.
2020/0142049 A1 5/2020 Solodky et al.
2020/0158861 A1 5/2020 Cattle et al.
2020/0191939 A1 6/2020 Wu et al.
2020/0292666 A1 9/2020 Maher et al.
2020/0313719 A1 10/2020 Blanchard et al.
2020/0363499 A1 11/2020 Mayer et al.
2020/0393536 A1 12/2020 Stettiner
2021/0181300 A1 6/2021 Choi et al.
2021/0190904 A1 6/2021 Bourdoux et al.
2021/0190905 A1 6/2021 Roger et al.
2021/0364634 A1 11/2021 Davis et al.
2021/0389414 A1 12/2021 Behrens et al.
2022/0291335 A1 9/2022 Maher et al.
2022/0350020 A1 11/2022 Davis et al.
2022/0365169 A1 11/2022 Lefevre et al.

FOREIGN PATENT DOCUMENTS

EP 0725480 11/2011
EP 2374217 4/2013
EP 2884299 6/2015
EP 2821808 7/2015
EP 3349038 7/2018
EP 3062446 9/2018
EP 3152956 3/2019
EP 3483622 5/2019
EP 3499264 1/2020
FR 2751086 1/1998
GB 2529029 2/2016
JP 3625307 12/2004
JP 2010243330 10/2010
KR 101010522 1/2011
KR 102088426 12/2020
WO WO2008022981 2/2008
WO WO2010/022156 2/2010
WO WO2012115518 8/2012
WO WO2013147948 10/2013
WO WO2015175078 11/2015
WO WO2015185058 12/2015
WO WO2016011407 1/2016
WO WO2016030656 3/2016
WO WO2017187242 2/2017
WO WO2017059961 4/2017
WO WO2017175190 10/2017
WO WO2017187330 11/2017
WO WO2020/259916 12/2020

OTHER PUBLICATIONS

Fraser, "Design and simulation of a coded sequence ground penetrating radar," In: Diss. University of British Columbia, Dec. 3, 2015.

Zhou et al., "Linear extractors for extracting randomness from noisy sources," In: Information Theory Proceedings (ISIT), 2011 IEEE International Symposium on Oct. 3, 2011.

V. Giannini et al., "A 79 GHz Phase-Modulated 4 Ghz-Bw Cw Radar Transmitter in 28 nm CMOS,"in IEEE Journal of Solid-State Circuits, vol. 49, No. 12, pp. 2925-2937, Dec. 2014. (Year: 2014).

Óscar Faus García, "Signal Processing for mm Wave MIMO Radar," University of Gavle, Faculty of Engineering and Sustainable Development, Jun. 2015; Retrieved from the Internet from http://www.diva-portal.se/smash/get/diva2:826028/FULLTEXT01.pdf.

(56) **References Cited**

OTHER PUBLICATIONS

Levanan Nadav et al., "Non-coherent pulse compression—aperiodic and periodic waveforms", IET Radar, Sonar & Navagation, The Institution of Engineering and Technology, Jan. 1, 2016, pp. 216-224, vol. 10, Iss. 1, UK.

Akihiro Kajiwara, "Stepped-FM Pulse Radar for Vehicular Collision Avoidance", Electronics and Communications in Japan, Part 1, Mar. 1998, pp. 234-239, vol. 82, No. 6 1999.

A. Bourdoux, U. Ahamd, D. Guermandi, S. Brebels, A. Dewilde, W. Van Thillo, PMCW "Waveform and MIMO Technique for a 79 GHz CMOS Automotive Radar", 2016 IEEE Radar Conference (RadarConf), 2016, pp. 1-5, doi: 10.1109/RADAR.2016.7485114. (Year: 2016).

V. Jain, F. Tzeng, L. Zhou and p. Heydari, "A single-Chip Dual-Band 22-29-GHz/77-81-GHz BiCMOS Transceiver for Automotive Radars," in IEEE Journal of Solid-State Circuits, vol. 44, No. 12, pp. 3469-3485, Dec. 2009, doi: 10.1109/JSSC.2009.2032583. (Year: 2009).

A. Medra et al., "An 80 GHz Low-Noise Amplifier Resilient to the TX Spillover in Phase-Modulated Continuous-Wave Radars," in IEEE Journal of Solid-State Circuits, vol. 51, No. 5, pp. 1141-1153, May 2016, doi: 10.1109/JSSC.2016.2520962. (Year: 2016).

B. P. Ginsburg et al., "A multimode 76-to-81Ghz automotive radar transceiver with autonomous monitoring," 2018 IEEE International Solid—State Circuits Conference—(ISSCC), 2018, pp. 158-160, doi: 10.1109/ISSCC.2018.8310232 (Year: 2018).

Y. Ma, C. Miao, Y. Zhao, and W. Wu, " An MIMO Radar System Based on the Sparse-Array and Its Frequency Migration Calibration Method", in MDPI Journal of Sensors, vol. 19, issue No. 16, Published Aug. 2019, doi: 10.3390/s19163580 (Year: 2019).

RadarRangeEquation2011.pdf from http://www.ece.uah.edu/courses/material/EE619-2011/RadarRangeEquation(2)2011.pdf (Year: 2011).

What are S-Parameters Everything RF.pdf from https://www.everythingrf.com/community/what-are-s-parameters (Year 2018).

* cited by examiner

FIG. 1A

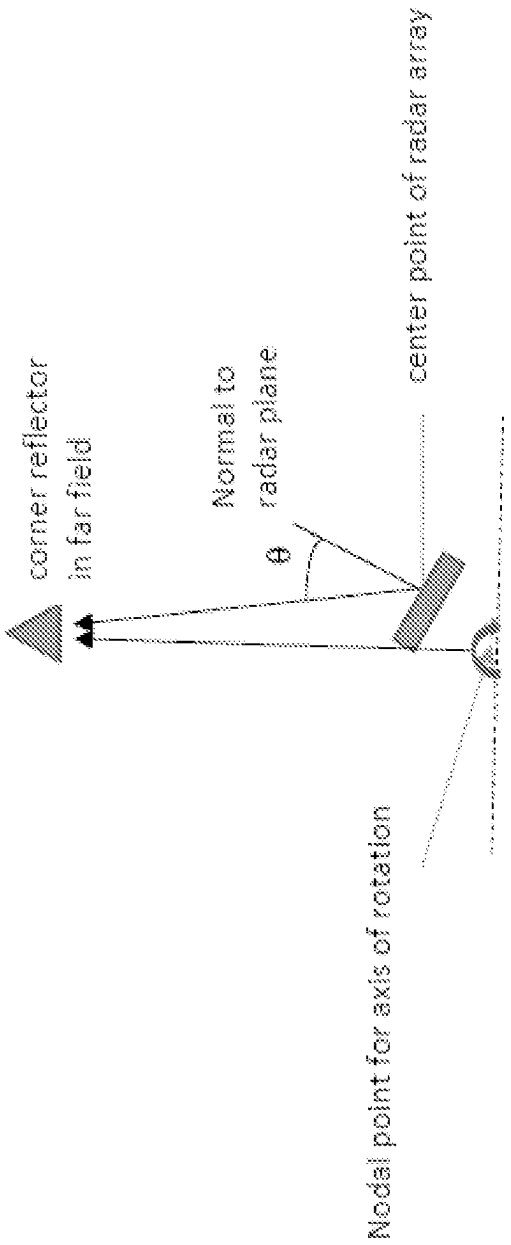
corner reflector
in far field
Normal to
radar plane
θ
center point of radar array
Nodal point for axis of rotation

FIG. 1B

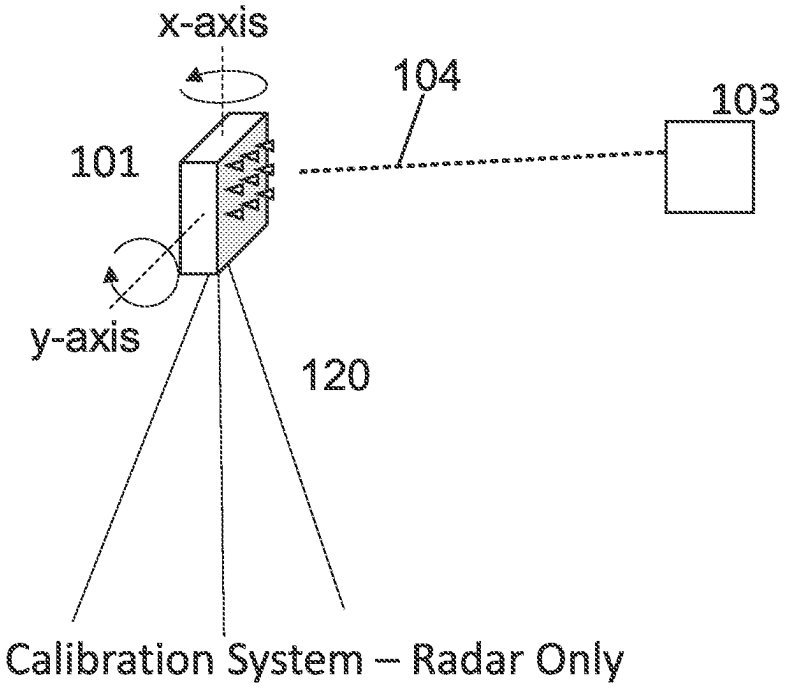

FIG. 1C

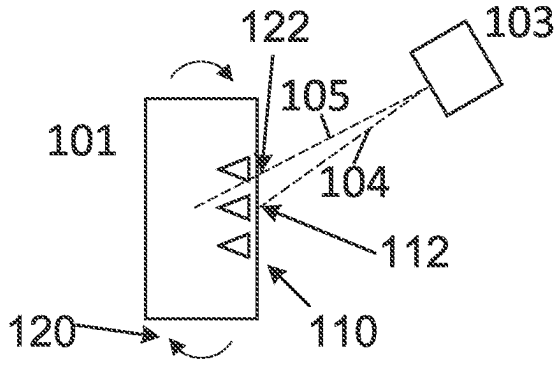

When nodal point for axis of rotation does not match the radar array center

FIG. 2

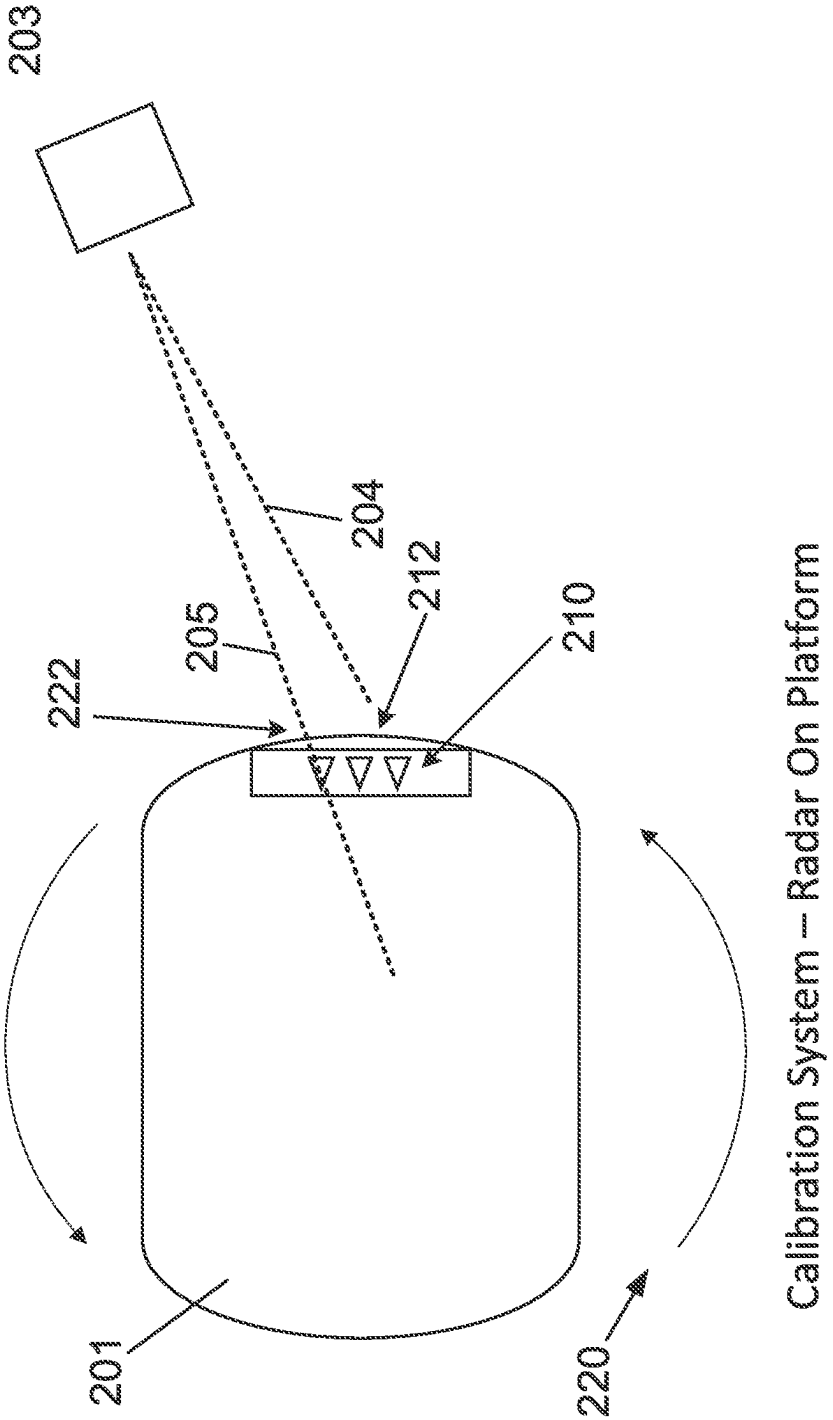
203
204
212
205
210
222
201
220
Calibration System – Radar On Platform

FIG. 3A

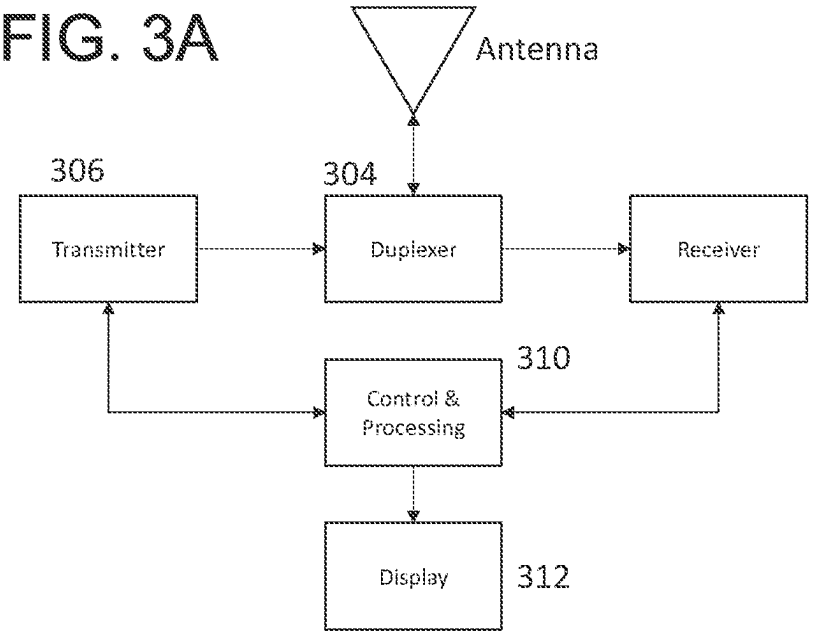
Antenna
306
304
Transmitter
Duplexer
Receiver
310
Control & Processing
Display
312

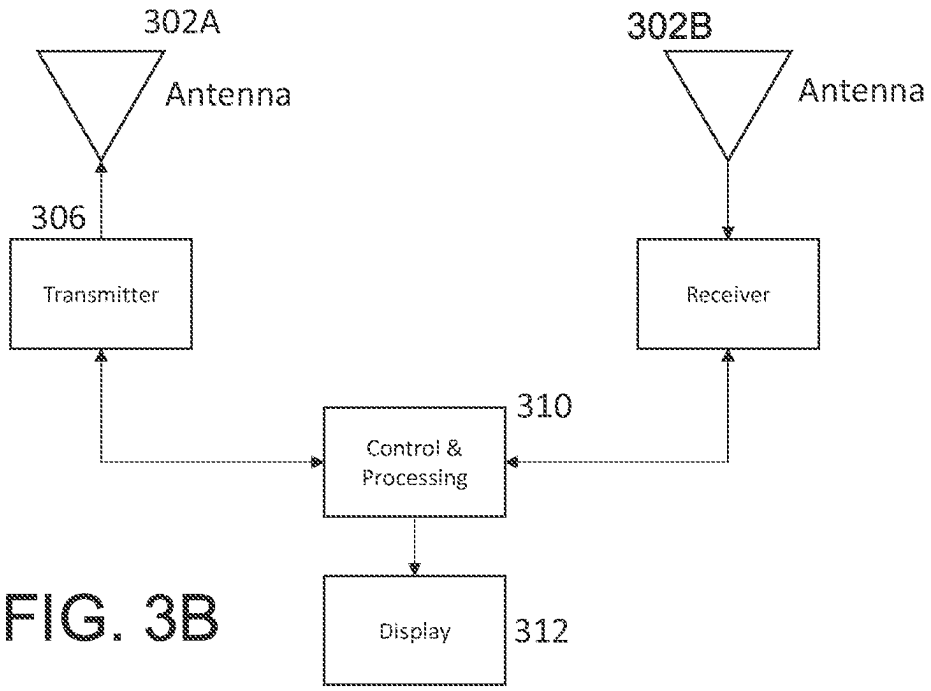
302A
Antenna
302B
Antenna
306
Transmitter
Receiver
310
Control & Processing
Display
312

FIG. 3B

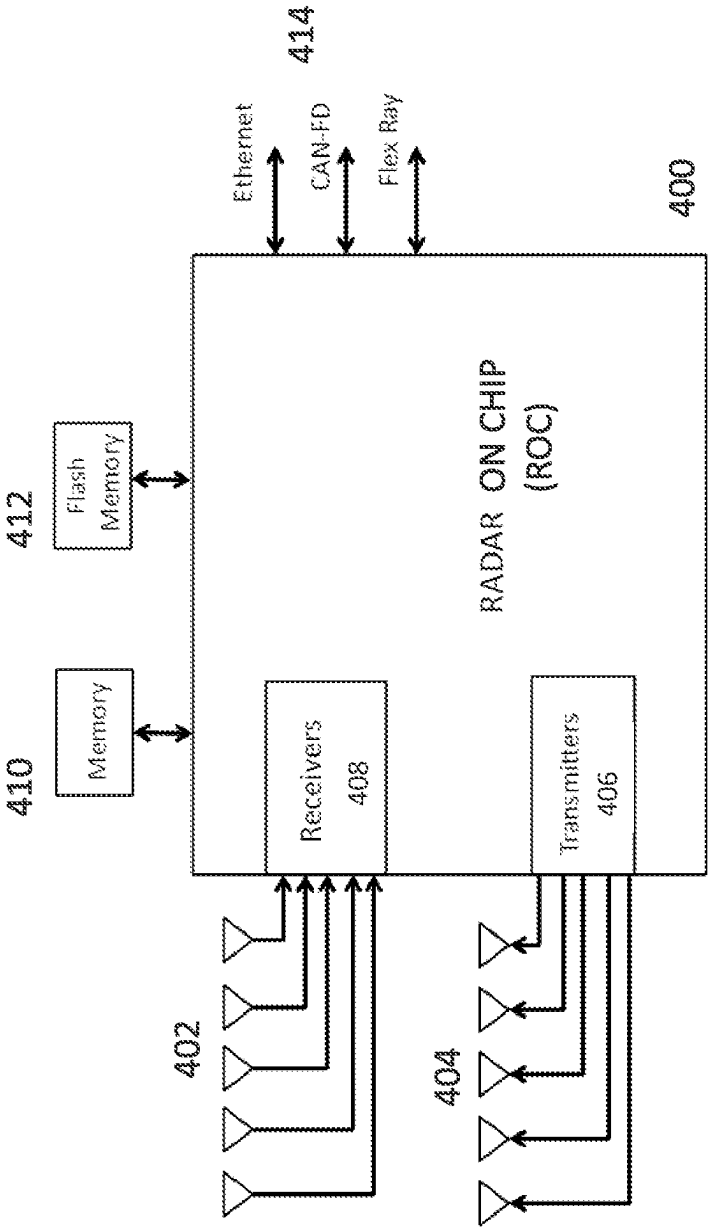
414
Ethernet
CAN-FD
Flex Ray
400
RADAR ON CHIP
(ROC)
412
Flash Memory
410
Memory
Receivers
408
Transmitters
406
402
404

FIG. 4

FIG. 5

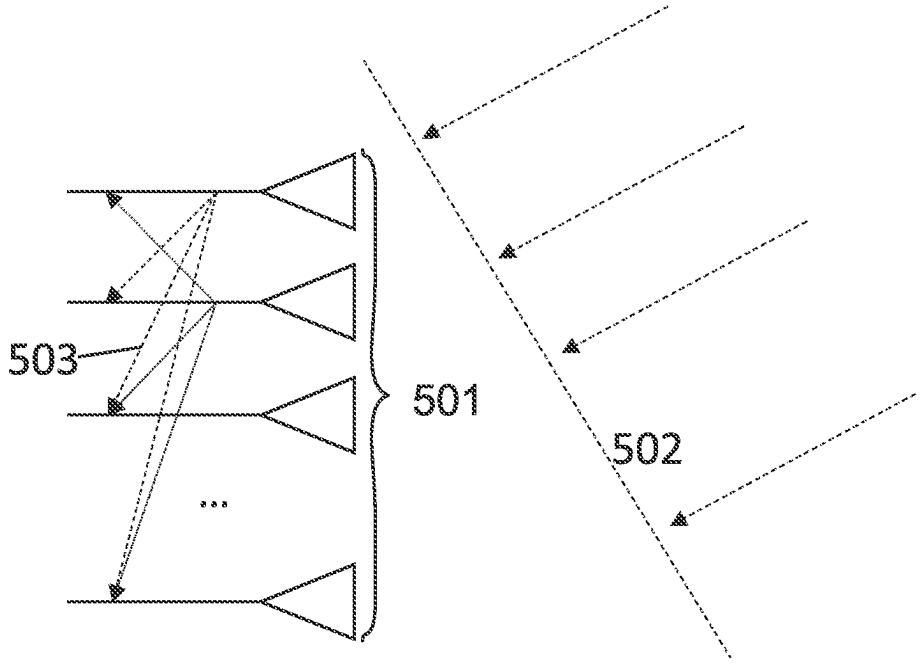

Cross Coupling

FIG. 6

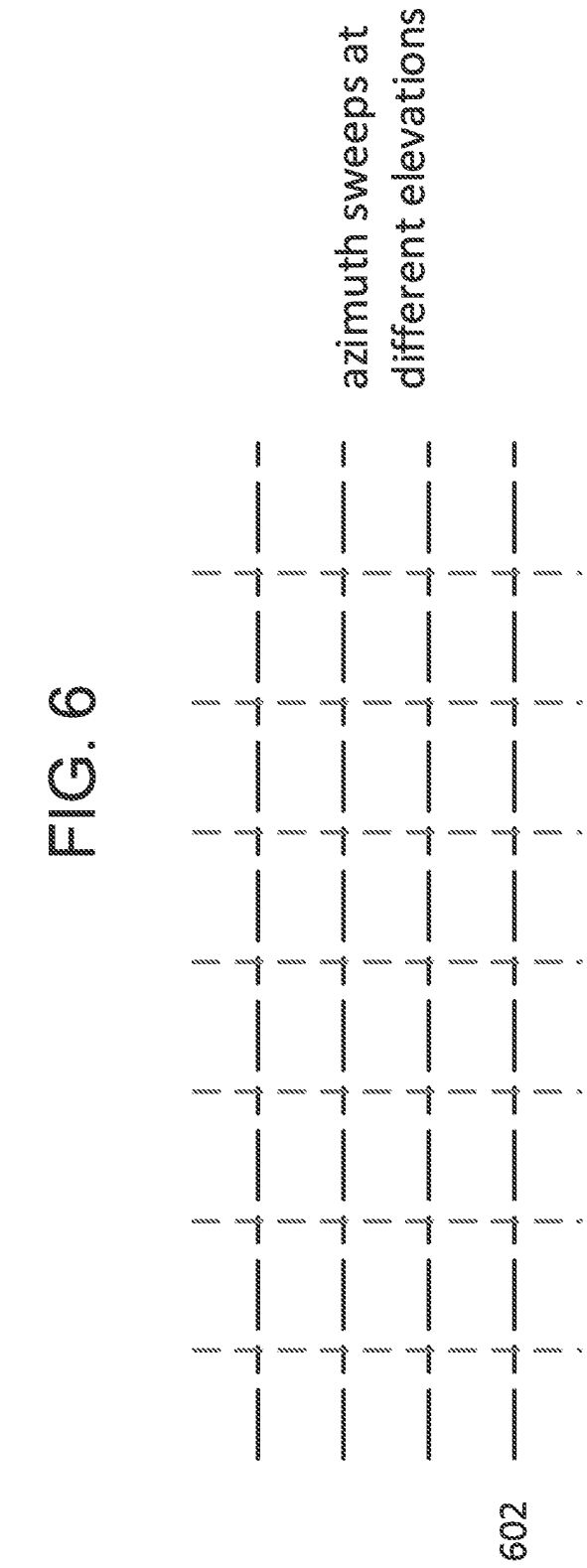
azimuth sweeps at different elevations
602
601
elevation sweeps at different azimuths
Sweep Patterns

FIG. 7

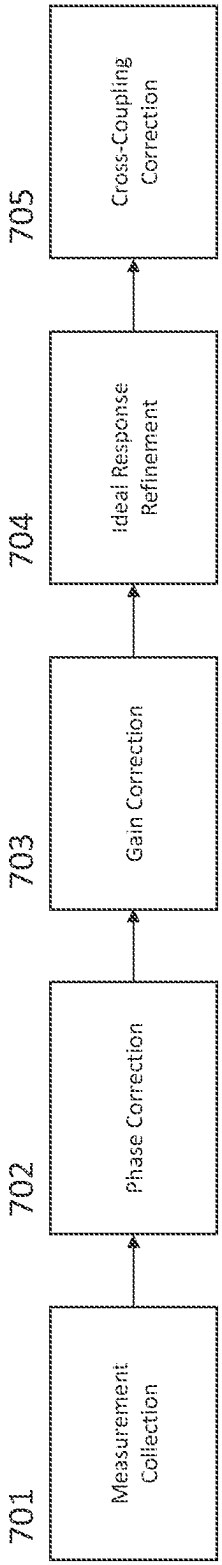
701
Measurement Collection
702
Phase Correction
703
Gain Correction
704
Ideal Response Refinement
705
Cross-Coupling Correction

FIG. 8: Phase Correction

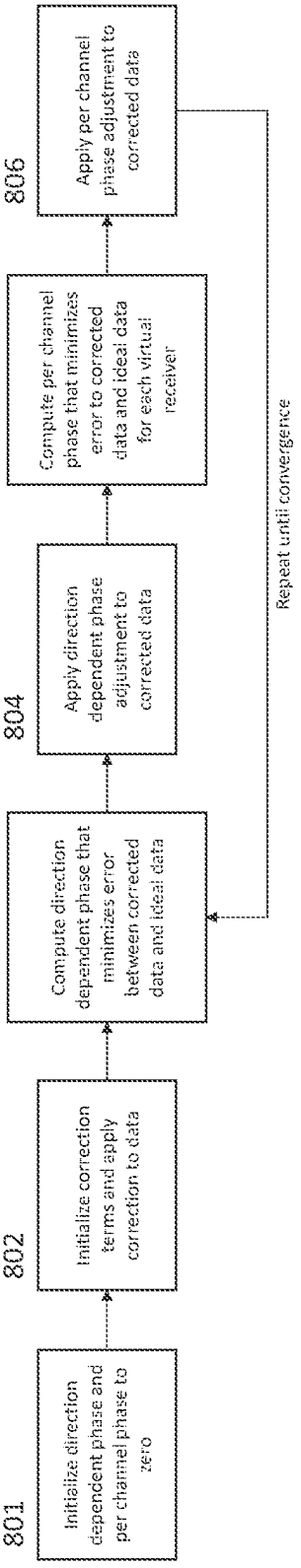

FIG. 9: Gain Correction

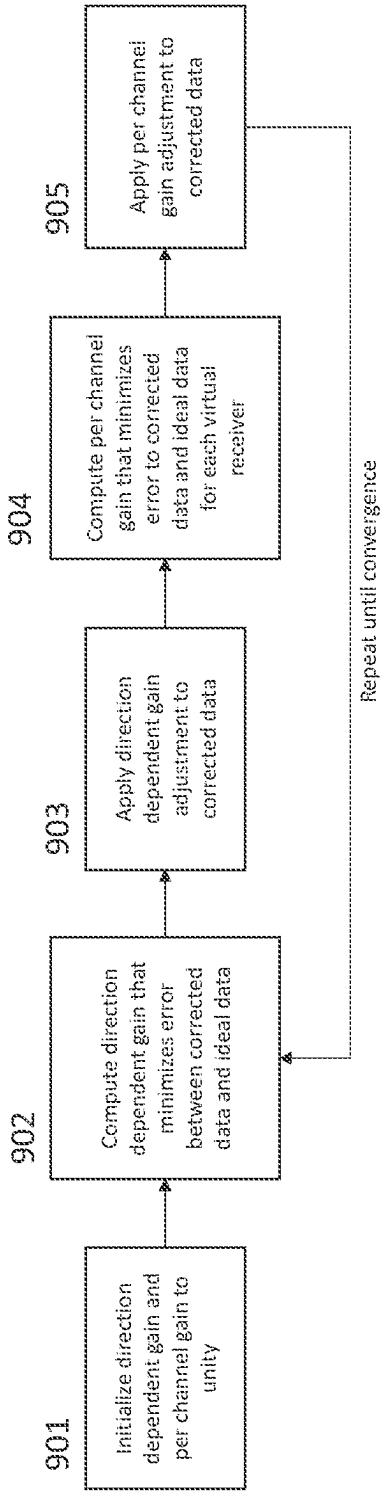

FIG. 10: Cross-Coupling Correction

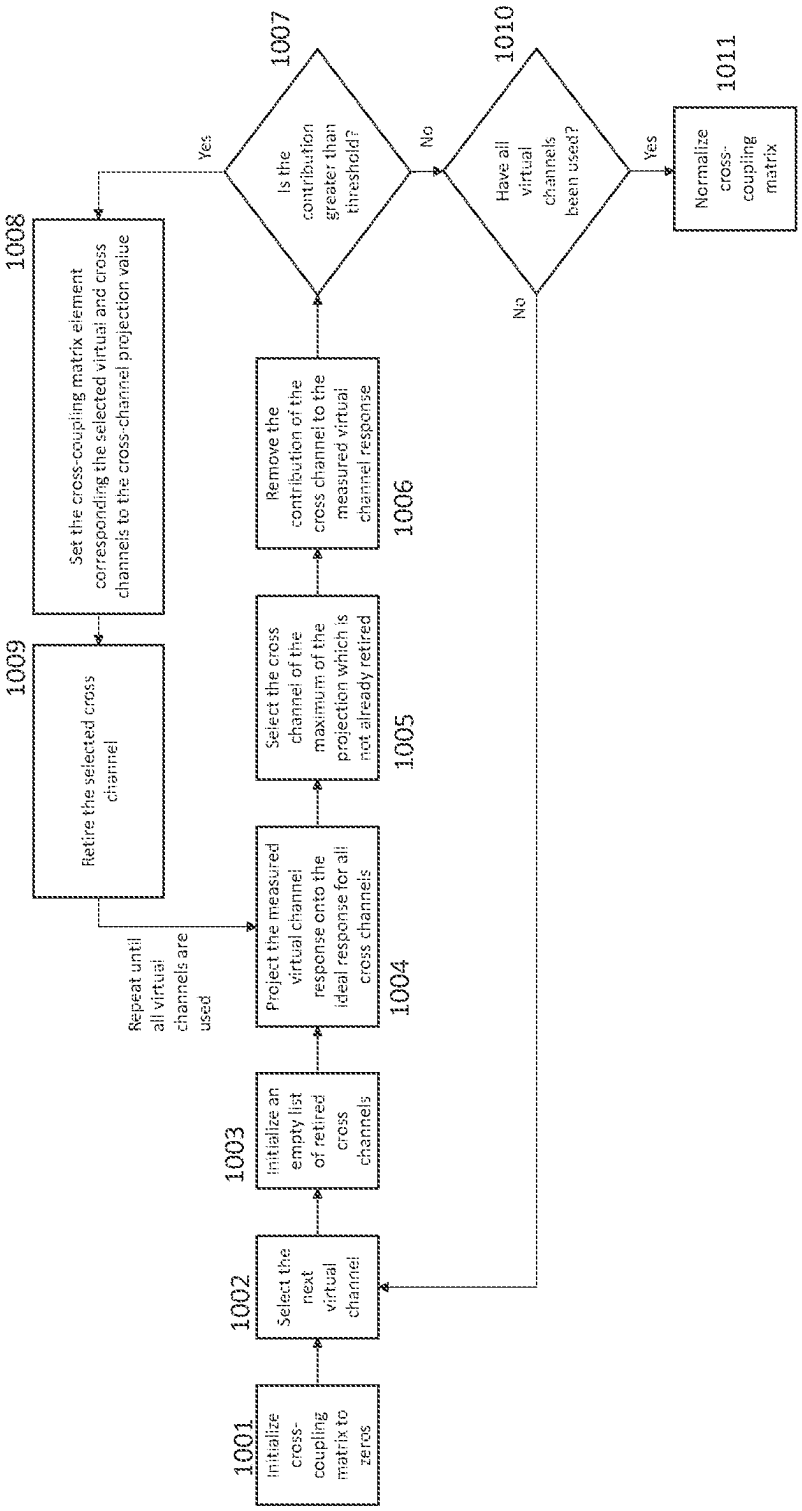

METHOD AND SYSTEM FOR ANTENNA ARRAY CALIBRATION FOR CROSS-COUPLING AND GAIN/PHASE VARIATIONS IN RADAR SYSTEMS

CROSS REFERENCE TO RELATED APPLICATION

The present application claims priority to and is a continuation of U.S. patent application Ser. No. 17/147,914, filed Jan. 13, 2021, which claims the benefits of U.S. provisional application, Ser. No. 62/960,220, filed Jan. 13, 2020, which are hereby incorporated by reference herein in their entireties.

The present invention is directed to radar systems, and more particularly to radar systems for vehicles and robotics.

BACKGROUND OF THE INVENTION

The use of radar to determine location, range, and velocity of objects in an environment is important in a number of applications including automotive radar, industrial processes, robotic sensing, gesture detection, and positioning. A radar system typically transmits radio signals and listens for the reflection of the radio signals from objects in the environment. By comparing the transmitted radio signals with the received radio signals, a radar system can determine the distance to an object, and the velocity of the object. Using multiple transmitters and/or receivers, or a movable transmitter or receiver, the location (angle) of an object can also be determined. Therefore, radar systems require accurate operation to maintain their optimal performance.

SUMMARY OF THE INVENTION

Embodiments of the present invention provide for a radar calibration system that calibrates for radar system impairments using a series of radar data measurements. Such impairments include coupling effects, per channel gain and phase variations, and direction dependent gain and phase variations. This calibration system operates under a variety of environments, with a variety of external information, and with a variety of objective functions to modify the measurement collection as well as the calibration processing to optimize the system with respect to a given objective function.

In an aspect of the present invention, a radar system for a robot or vehicle that calibrates for system impairments includes a radar system with at least one transmitter and at least one receiver. The transmitter and receiver are connected to at least one antenna. The transmitter is configured to transmit radio signals. The receiver is configured to receive a radio signal that includes the transmitted radio signal transmitter by the transmitter and reflected from objects in the environment. The receiver is also configured to receive radio signals transmitted by other radar systems.

In an aspect of the present invention, the radar system comprises one of: a single transmitter and a plurality of receivers; a plurality of transmitters and a single receiver; and a plurality of transmitters and a plurality of receivers.

In a further aspect of the present invention, the transmitters and receivers may be connected to multiple antennas through a switch.

In another aspect of the present invention, the radar system includes a calibration module that is configured to rotate its direction in both azimuth and elevation. In the presence of at least one reflecting object, the calibration module collects reflected signals from the at least one reflecting object at desired angles of interest in the azimuth and elevation space. This rotation may occur in either a continuous manner or a discrete "stop-and-go" manner. The radar system's center point of the antenna array does not need to align with the center point of rotation, and the radar system corrects for phase distortion and angle-of-arrival error due to this misalignment. This misalignment is referred to as nodal displacement. The calibration module then processes these measurements into a correction matrix, which calibrates for radar system impairments. These may include phase error due to nodal displacement, per channel phase variation, direction dependent phase variation, per channel amplitude variation, direction dependent amplitude variation, and channel response cross coupling. The angles-of-arrival of the collected reflected signals may be either estimated by the radar system or determined through prior knowledge of the object(s) location(s) relative to the radar system.

In another aspect of the present invention, the radar system may modify its measurement collection and calibration processing to optimize different objective functions. These modifications include the speed and manner of rotation, quantity of measurements collected, and the selection of antenna(s) and channel(s) transmitting and receiving the signal(s). These modifications also include parameters in the processing that control the computation of the correction matrix and affect the processing speed and correction accuracy.

In another aspect of the present invention, a method for calibrating a radar system for system impairments includes at least one transmitter transmitting radio signals. At least one receiver is receiving radio signals that include radio signals transmitted by the transmitter and reflected from objects in an environment. The at least one transmitter and the at least one receiver are coupled to an antenna array. A platform rotating the at least one receiver and the at least one transmitter in both azimuth and elevation. An array center of the antenna array is not aligned with the platform's rotational center. The method includes collecting, with a calibration module, in the in the presence of at least one object, reflected signals from the at least one object at desired angles of interest in azimuth and elevation, calculating a misalignment between the array center of the antenna array and the rotation center of the platform. The method also includes correcting, with the at least one receiver, for phase distortion and angle-of-arrival error due to the calculated misalignment. The misalignment between the array center of the antenna and the rotation center of the platform is a nodal displacement. The array center of the antenna array is a nodal point.

These and other objects, advantages, purposes and features of the present invention will become apparent upon review of the following specification in conjunction with the drawings.

BRIEF DESCRIPTION OF THE DRAWINGS

FIG. **1**A is a diagram of a radar system where a nodal point for an axis of rotation does not match a radar array center of the radar system in accordance with the present invention;

FIG. **1**B is a perspective view of a radar calibration system orientated towards a target in accordance with the present invention;

FIG. **1**C is another view of the radar calibration system and target of FIG. **1**B;

FIG. **2** is a diagram of a radar calibration system installed on a maneuverable platform in accordance with the present invention;

FIG. **3**A and FIG. **3**B are block diagrams of radar systems that use the calibration system in accordance with the present invention;

FIG. **4** is a block diagram illustrating a radar with a plurality of receivers and a plurality of transmitters (MIMO radar) that uses the calibration system in accordance with the present invention;

FIG. **5** is a visualization of an exemplary antenna array, an exemplary received plane wave, and exemplary coupling effects in accordance with the present invention;

FIG. **6** is a diagram of exemplary sweep patterns executed during an exemplary measurement procedure in accordance with the present invention;

FIG. **7** is a flow chart describing the high-level processes of the calibration procedure, in accordance with the present invention;

FIG. **8** is a flow chart describing the process of estimating direction dependent and per channel phase correction, in accordance with the present invention;

FIG. **9** is a flow chart describing the process of estimating direction dependent and per channel gain correction, in accordance with the present invention; and

FIG. **10** is a flow chart describing the process of estimating cross-coupling correction, in accordance with the present invention;

DESCRIPTION OF THE PREFERRED EMBODIMENTS

Referring to the drawings and the illustrative embodiments depicted therein, wherein numbered elements in the following written description correspond to like-numbered elements in the figures, a calibration system provides for a calibration of a radar system. The radar system includes a calibration module that includes a platform for rotating receivers and transmitters of the radar system in both azimuth and elevation. An array center of the antenna array is not aligned with the platform's rotational center. The calibration module collects, in the presence of at least one object, reflected signals from the at least one object at desired angles of interest in azimuth and elevation. The calibration module calculates a misalignment between the array center of the antenna array and the rotation center of the platform. The at least one receiver corrects for phase distortion and angle-of-arrival error due to the calculated misalignment. The misalignment between the array center of the antenna and the rotation center of the platform is a nodal displacement. The array center of the antenna array is a nodal point.

An exemplary radar system operates by transmitting one or more signals from one or more transmitters and then listening for reflections of those signals from objects in the environment by one or more receivers. By comparing the transmitted signals and the received signals, estimates of the range, velocity, and angle (azimuth and/or elevation) of the objects can be estimated.

There are several different types of signals that transmitters in radar systems employ. A radar system may transmit a pulsed signal or a continuous signal. In a pulsed radar system, the signal is transmitted for a short time and then no signal is transmitted. This is repeated over and over. When the signal is not being transmitted, the receiver listens for echoes or reflections from objects in the environment. Often a single antenna is used for both the transmitter and receiver and the radar transmits on the antenna and then listens to the received signal on the same antenna. This process is then repeated. In a continuous wave radar system, the signal is continuously transmitted. There may be an antenna for transmitting and a separate antenna for receiving.

Another classification of radar systems is the modulation of signal being transmitted. A first type of continuous wave radar signal is known as a frequency modulated continuous wave (FMCW) radar signal. In an FMCW radar system, the transmitted signal is a sinusoidal signal with a varying frequency. By measuring a time difference between when a certain frequency was transmitted and when the received signal contained that frequency, the range to an object can be determined. By measuring several different time differences between a transmitted signal and a received signal, velocity information can be obtained.

A second type of continuous wave signal used in radar systems is known as a phase modulated continuous wave (PMCW) radar signal. In a PMCW radar system, the transmitted signal from a single transmitter is a sinusoidal signal in which the phase of the sinusoidal signal varies. Typically, the phase during a given time period (called a chip period or chip duration) is one of a finite number of possible phases. A spreading code consisting of a sequence of chips, (e.g., +1, +1, −1, +1, −1 . . .) is mapped (e.g., +1→0, −1→□) into a sequence of phases (e.g., 0, 0, □, 0, □ . . .) that is used to modulate a carrier to generate the radio frequency (RF) signal. The spreading code could be a periodic sequence or could be a pseudo-random sequence with a very large period so it appears to be a nearly random sequence. The spreading code could be a binary code (e.g., +1 or −1). The resulting signal has a bandwidth that is proportional to the rate at which the phases change, called the chip rate R_c, which is the inverse of the chip duration, $T_c=1/R_c$. By comparing the return signal to the transmitted signal, the receiver can determine the range and the velocity of reflected objects.

In some radar systems, the signal (e.g. a PMCW signal) is transmitted over a short time period (e.g. 1 microsecond) and then turned off for a similar time period. The receiver is only turned on during the time period where the transmitter is turned off. In this approach, reflections of the transmitted signal from very close targets will not be completely available because the receiver is not active during a large fraction of the time when the reflected signals are being received. This is called pulse mode.

Digital frequency modulated continuous wave (FMCW) and phase modulated continuous wave (PMCW) are techniques in which a carrier signal is frequency or phase modulated, respectively, with digital codes using, for example, GMSK. Digital FMCW radar lends itself to be constructed in a MIMO variant in which multiple transmitters transmitting multiple codes are received by multiple receivers that decode all codes.

The advantage of the MIMO digital FMCW radar is that the angular resolution is that of a virtual antenna array having an equivalent number of elements equal to the product of the number of transmitters and the number of receivers. Digital FMCW MIMO radar techniques are described in U.S. Pat. Nos. 9,989,627; 9,945,935; 9,846,228; and 9,791,551, which are all hereby incorporated by reference herein in their entireties.

The radar sensing system of the present invention may utilize aspects of the radar systems described in U.S. Pat. Nos. 10,261,179; 9,971,020; 9,954,955; 9,945,935; 9,869,762; 9,846,228; 9,806,914; 9,791,564; 9,791,551; 9,772,397; 9,753,121; 9,689,967; 9,599,702; 9,575,160, and/or 9,689,967, and/or U.S. Publication Nos. US-2017-0309997;

and/or U.S. patent application Ser. No. 16/674,543, filed Nov. 5, 2019, Ser. No. 16/259,474, filed Jan. 28, 2019, Ser. No. 16/220,121, filed Dec. 14, 2018, Ser. No. 15/496,038, filed Apr. 25, 2017, Ser. No. 15/689,273, filed Aug. 29, 2017, Ser. No. 15/893,021, filed Feb. 9, 2018, and/or Ser. No. 15/892,865, filed Feb. 9, 2018, and/or U.S. provisional application, Ser. No. 62/816,941, filed Mar. 12, 2019, which are all hereby incorporated by reference herein in their entireties.

Antenna Calibration:

Determining a correct angle calibration matrix to counter the impact of effective cross-coupling between virtual receivers in large-scale MIMO systems has been challenging. The problem is especially acute when the system is large or cannot be conveniently placed on the rotating measurement system. In some cases, a nodal point cannot be maintained or cannot even be accurately determined. Such cases occur in radars mounted on robots, drones or other devices, or in cases when angle calibration is desired in situ with the whole system assembled. An exemplary method is disclosed that efficiently and correctly determines channel-to-channel variations and cross-coupling coefficients from angle sweep data in the presence of an unknown nodal point of the system. An exemplary algorithm also produces the diagonal calibration values as a by-product.

Typical angle calibration methods require collection of channel response data for a number of angles, which is also called as angle sweep data. The data is collected in an anechoic chamber with a single target in far-field and radar mounted on a gimbal that can be rotated between the angles of interest (up-to ±90 degrees), which allows collecting the target virtual channel response in those angles. A typical data collection system is shown in FIG. **1**A. This represents the case where the nodal point for the axis of rotation is the same as the center of the radar antenna system. The radar may have planar antenna array (2-D) instead of a linear antenna array (1-D). The radar will then need to rotate in two axes maintaining the nodal point of rotation in both axes at the center of the planar antenna array. The antenna array can be a virtual array created through the use multi-input multi-output (MIMO) technology.

FIGS. **1**B and **1**C illustrate an exemplary calibration system for a radar system. As discussed herein, the calibration system and radar system is first installed in a temporary installation. While in the temporary installation, the calibration system records calibration measurements. The calibration system is capable of recording a series of calibration measurements. Henceforth, an exemplary "measured channel response" refers to the data from these calibration measurements. As illustrated in FIGS. **1**B and **1**C, a radar **101** is mounted on top of an adjustable gimbal mount platform (hereinafter a "platform") **120**. The platform **120** is configured to rotate in one or both of azimuth (x-axis) and elevation (y-axis). The radar **101** is configured to transmit a signal to a reflecting object **103**. FIGS. **1**B and **1**C illustrate a signal traversal path **104** extending from an array center **112** of an antenna array **110** to the reflecting object **103**, while an expected path **105** is illustrated from the platform's rotation center **122** to the reflecting object **103**. The deviance in angle between the signal traversal path **104** and the expected path **105** causes a phase shift between the expected signal **105** and the actual reflected signal **104**, as well as an error in the angle of arrival. This deviance is referred to as nodal displacement, and the phase shift is modeled as a direction dependent phase variation. Nodal displacement occurs for multiple of reasons. First, the height of the radar **101** on the platform **120** may not exactly match the plane of the nodal point of rotation. Second, the nodal point may not exactly match the virtual center of the antenna array. The radar **101** may also have multiple antenna configurations with different virtual centers, and physical relocation of the radar system **101** may not be feasible. Last, there can be an error in estimating the correct nodal point.

FIG. **2** illustrates an exemplary radar/calibration system **201** which records calibration measurements while the radar/calibration system **201** is installed in a final platform or rotatable gimbal (the "platform") **220**. As illustrated in FIG. **2**, the radar/calibration system **201** is mounted in the platform **220**. A reflecting object **203** is positioned in front of the radar/calibration system **201**. FIG. **2** illustrates a signal traversal path **204** extending from an array center **212** of an antenna array **210** of the radar **201** to a reflecting object **203**. An expected path **205** is also illustrated extending from the rotation axis **222** of the platform **220** to the reflecting object **203**. Rotation is achieved by the mechanics of the platform **220** itself. As in the previous paragraph, a direction dependent phase variation occurs due to nodal displacement when the rotation axis **222** of the platform **220** does not match the array center **212** of the antenna array **210**.

FIG. **3**A illustrates an exemplary radar using the calibration method and calibration system described in the current invention with at least one antenna **302** that is time-shared between at least one transmitter **306** and at least one receiver **308** via at least one duplexer **304**. Output from the receiver(s) **308** is received by a control and processing module **310** that processes the output from the receiver(s) **308** to produce display data for the display **312**. The control and processing module **310** is also operable to produce a radar data output that is provided to other control and processing units. The control and processing module **310** is also operable to control the transmitter(s) **306** and the receiver(s) **308**.

FIG. **3**B illustrates an alternative exemplary radar using the calibration method and system described in the current invention with separate sets of transmitter and receiver antennas. As illustrated in FIG. **3**B, at least one antenna **302**A for the at least one transmitter **306** and at least at least one antenna **302**B for the at least one receiver **308**.

FIG. **4** illustrates an exemplary MIMO (Multi-Input Multi-Output) radar **400** that is configured to use the calibration method and system described herein. With MIMO radar systems **400**, each transmitter signal is rendered distinguishable from every other transmitter signal by using appropriate differences in the modulation, for example, different digital code sequences. Each receiver **408** correlates with each transmitter signal, producing a number of correlated outputs equal to the product of the number of receivers **408** with the number of transmitters **406** (virtual receivers=RX_N*TX_N). The outputs are deemed to have been produced by a number of virtual receivers, which can exceed the number of physical receivers **408**.

FIG. **4** illustrates a radar system **400** with a plurality of antennas **402** connected to a plurality of receivers **408**, and a plurality of antennas **404** connected to a plurality of transmitters **406**. The radar system **400** of FIG. **4** is also a radar-on-chip system **400** where the plurality of receivers **408** and the plurality of transmitters **406**, along with any processing to produce radar data output and any interface (like Ethernet, CAN-FD, Flex Ray etc.), are integrated on a single semiconductor IC (Integrated Circuit). Using multiple antennas allows the radar system **400** to determine the angle of objects/targets in the environment. Depending on the geometry of the antenna system **402**, **404**, different angles (e.g., with respect to the horizontal or vertical) can be determined. The radar system **400** may be connected to a

network via an Ethernet connection or other types of network connections **414**. The radar system **400** may also include memory **410**, **412** to store software used for processing the received radio signals to determine range, velocity, and location of objects/targets in the environment. Memory may also be used to store information about objects/targets in the environment.

In practice, antenna elements have a directional gain and phase response. This response varies with respect to azimuth and elevation. The combination of transmitter and receiver antenna responses can be modeled as a new virtual antenna response. This response causes a gain and phase variation from the ideal signals at the virtual receivers. This effect can be divided into a per channel gain, per channel phase, direction dependent gain, and direction dependent phase.

In practice, leakage exists between antenna elements due to coupling effects. This coupling occurs between both the signals at the TX antenna elements and the RX antenna elements. This causes a deviation in both the signals that are transmitted by the transmitters **406** of the radar system **400** and the signals that are received by the receivers **408** of the radar system **400**. The combined effect of coupling at both the transmitter and the receiver is modeled as coupling between virtual receivers. FIG. **5** illustrates the coupling in a virtual array. FIG. **5** illustrates a virtual antenna element array **501**, a propagation front **502** of a far-field signal, and the path **503** of the signals to the virtual receivers. The signals at each virtual antenna element will couple. This coupling causes a gain and phase variation from the ideal signal at the virtual receivers. This impairment is henceforth referred to as mutual coupling.

In the preferred embodiment, the measured channel response is collected using a PMCW radar. Alternative embodiments may include other radar types.

Using the radar calibration systems described either in FIG. **1** or **2**, one method of collecting the calibration measurements is a stop and go sweep. In this method, the radar system is rotated to the exact desired azimuth and elevation angles, where it stops before collecting the radar data. This method provides increased accuracy.

A second method of collecting the calibration measurements is a continuous sweep. In this second method, the radar system rotates in a continuous fashion and collects radar data while rotating. This method provides increased speed. However, it sacrifices accuracy due to angular smearing of the target response. There is no doppler impact since the rotation causes the effective target movement to be tangential to the radar. FIG. **6** illustrates exemplary sweep patterns. FIG. **6** illustrates azimuth sweeps **601** and elevation sweeps **602**. The quantity, speed, and angular range of the sweeps is variable and chosen dependent on the array design. All sweeps contain a stationary measurement at boresight of the radar.

FIG. **7** illustrates the steps to an exemplary radar system calibration procedure. In step **701**, an exemplary measurement collection process is carried out. In step **702**, an exemplary phase correction process is carried out, which estimates and corrects for the per channel phase variation and direction dependent phase variation in the collected data. In step **703**, an exemplary gain correction process is carried out, which estimates and corrects for the per channel gain variation and direction dependent gain variation in the phase-corrected data. In step **704**, an exemplary ideal response refinement process is carried out, which uses the gain- and phase-corrected data to improve the angle-of-arrival estimation for the collected radar data. In step **705**, an exemplary cross-coupling calibration process is carried out, which estimates and corrects for the cross-coupling effects remaining in the gain- and phase-corrected data.

The radar data is described by the following exemplary mathematical model. Denoting az and el as the azimuth and elevation angles (in radians) to the target, define the u-v space as:

$$u = \sin(az)\cos(el)$$

$$v = \sin(el)$$

Assuming a planar antenna array where the k^{th} (out of N_{vrx}) virtual antenna is located at (0, dy_k, dz_k) in rectangular coordinates, the ideal receive data in the absence of any cross-coupling and no gain/phase variation is given by:

$$y_{ideal}(k, u, v) = e^{-j\frac{2\pi}{\lambda}(dy_k u + dz_k v)}$$

This ideal response of the N_{vrx} virtual antennas corresponding to a far-field target in the u and v (or equivalently in az and el) space is expressed in vector form as:

$$\vec{y}_{ideal}(u, v) = [y_{ideal}(0, u, v), y_{ideal}(1, u, v), \ldots, y_{ideal}(N_{vrx} - 1, u, v)]^T$$

In the presence of cross-coupling, the received signal vector is $\vec{x} = A\vec{y}_{ideal}$, where $A = \{a_{m,k}\}$, $0 \le m,k \le N_{vrx} - 1$ is a matrix that captures both coupling and per channel gain and phase variation. With this impairment, the received data becomes:

$$x(k, u, v) = \sum_{m=0}^{N_{vrx}-1} \alpha_{m,k} e^{-j\frac{2\pi}{\lambda}(dy_m u + dz_m v)}$$

The vector representation of the channel response $\vec{x}(u, v)$ is then:

$$\vec{x}(u, v) = [x(0, u, v), x(1, u, v), \ldots, x(N_{vrx} - 1, u, v)]^T$$

The data model described above applies to a far-field target. The embodiments of the method and calibration system discussed herein equally applies to a near-field target as well with a corresponding modification of the signal vectors defined above. The data model can be updated for non-nodal displacement for the radar in the data collection setup as follows:

$$x_{meas}(k, u, v) = \gamma(u, v) \sum_{m=0}^{N_{vrx}-1} \alpha_{m,k} e^{-j\frac{2\pi}{\lambda}(dy_m(u - \delta u(u,v)) + dz_m(v - \delta v(u,v)))}$$

Here, $\gamma(u, v)$ is due to the angle dependent phase correction (e.g., as a result of nodal displacement). $\delta u(u, v)$ and $\delta v(u, v)$ represent the angle dependent (hence the notation that these parameters are dependent on the

angle of incidence as well) mismatch between the expected direction and the actual sampled direction.

The vector representation $\vec{x}_{meas}$ (u, v) is:

$$\vec{x}_{meas}(u, v) = [x_{meas}(0, u, v), x_{meas}(1, u, v), \ldots, x_{meas}(N_{vrx} - 1, u, v)]^T$$

or

$$\vec{x}_{meas}(u, v) = \gamma(u, v)\vec{A}\vec{y}_{ideal}(u - \delta u(u, v), v - \delta v(u, v))$$

FIG. **8** illustrates an exemplary calibration procedure for direction dependent phase variation and per channel phase variation. In step **801**, the estimates of the direction dependent phase variation and per channel phase variation are initialized to zero. Then, in step **802**, a correction term is computed as the normalized complex conjugate of the measured channel response at boresight of the radar system. Then an iterative procedure begins. In step **803**, the direction dependent phase variation is estimated using least-squares to minimize the difference between the corrected channel response and the ideal channel response. In step **804**, the channel response is corrected again with this phase. Next in step **805**, the per channel phase variation is estimated using least-squares to minimize the difference between the corrected channel response and the ideal channel response, now across all directions. In step **806**, the channel response is corrected again with this phase. This iterative procedure is repeated for a fixed number of iterations or until convergence.

This phase calibration procedure can be described mathematically using the previous exemplary signal model. The initial coupling matrix in step **802** is set to zeros, except for the diagonal elements which are initially set to

$$a_{k,k}^{brs} = \frac{x_{meas}^*(k, 0, 0)}{|x_{meas}(k, 0, 0)|}$$

since $\vec{x}_{meas}$ (k, 0,0) is the channel measured at boresight on the k^{th} virtual element. Accordingly with step **801** and step **802**, we now initialize the following terms: direction dependent phase term: $\angle\tilde{\gamma}^0$ (u, v)=0, per channel phase term: $\angle\tilde{a}_{k,k}{}^0$=0, and the array response corrected for the direction dependent and per channel phase terms $\tilde{x}^0$ (k, u, v)=$a_{k,k}{}^{brs}x_{meas}$(k, u, v). Then the iterative procedure begins. The superscript it is the iteration index. The direction-dependent least squares solution, $\angle\tilde{\gamma}^{it}$(u, v), in step **803** is obtained by minimizing the cost function below:

$$C_{1,phase}(u, v) = \sum_{k=0}^{N_{vrx}-1} \left| y_{ideal}(k, u, v)e^{-j\angle\tilde{\gamma}^{it}(u,v)} - \tilde{x}^{it-1}(k, u, v) \right|^2$$

The radar data is then updated in step **804** as

$$\tilde{x}^{it}(k, u, v) = \tilde{x}^{it-1}(k, u, v)e^{j\angle\tilde{\gamma}^{it}(u,v)}$$

The per channel least squared solution, $\angle\tilde{a}_{k,k}{}^{it}$, in step **805** is obtained by minimizing the cost function below

$$C_{2,phase}(k) = \sum_{u,v} \left| y_{ideal}(k, u, v)e^{-j\angle\tilde{\alpha}_{k,k}^{it}} - \tilde{x}^{it}(k, u, v) \right|^2$$

The radar data is then updated in step **806** as

$$\tilde{x}^{it}(k, u, v) = \tilde{x}^{it}(k, u, v)e^{j\angle\tilde{\alpha}_{k,k}^{it}}$$

This procedure loops for a finite number of iterations. Let the number of iterations be L. At the end of iterations, we obtain the following information: updated virtual array response (corrected for phase which corrects for nodal displacement as well as phase response per angle) $\tilde{x}$(k, u, v)=$\tilde{x}^L$(k, u, v), estimate of direction dependent phase correction

$$\angle\tilde{\gamma}(u, v) = \Sigma_{it=1}^{L}\angle\tilde{\gamma}^{it}(u, v),$$

and estimate of per channel phase variation

$$\angle\tilde{\alpha}_{k,k} = \Sigma_{it=1}^{L}\angle\tilde{\alpha}_{k,k}^{it}.$$

FIG. **9** illustrates an exemplary calibration procedure for direction dependent gain variation and per channel gain variation. First in step **901**, the estimates of the direction dependent gain and per channel gain are initialized to unity. The corrected channel response after the phase correction is now used. Then an iterative procedure begins. In step **902**, the direction dependent gain is estimated using least-squares to minimize the difference between the corrected channel response and the ideal channel response. Note that the ideal channel response is unity across all virtual receivers. In step **903**, the channel response is corrected with this gain. Next in step **904**, the per channel gain is estimated using least-squares to minimize the difference between the corrected channel response and the ideal channel response, now across all directions. In step **905**, the channel response is corrected again with this gain. This iterative procedure is repeated for a fixed number of iterations or until convergence.

This gain calibration procedure can be described mathematically using the previous exemplary signal model. Accordingly, with step **901**, the following terms are initialized: direction dependent amplitude term: $|\tilde{\gamma}^0(u, v)|$=1, per channel amplitude term: $|\tilde{a}_{k,k}{}^0|$=1, and the array response as corrected at the output of the previous phase calibration stage $\tilde{x}^0$(k, u, v)=$\tilde{x}$(k, u, v). Then the iterative procedure begins. The direction-dependent least-squares solution, $|\tilde{\gamma}^{it}$ (u, v)|, in step **902**, is obtained by minimizing the cost function below:

$$C_{1,gain}(u, v) = \sum_{k=0}^{N_{vrx}-1} \| y_{ideal}(k, u, v)| |\tilde{\gamma}^{it}(u, v)| - \left|\tilde{x}^{it-1}(k, u, v)\right| \|^2$$

The radar data is then updated in step **903** as:

$$\tilde{x}^{it}(k, u, v) = \tilde{x}^{it-1}(k, u, v)\left|\tilde{\gamma}^{it}(u, v)\right|$$

The per channel least-squares solution, $|\tilde{a}_{k,k}^{it}|$, in step **904** is obtained by minimizing the cost function below

$$C_{2,gain}(k) = \sum_{u,v} \left| y_{ideal}(k, u, v) \left| \tilde{\alpha}_{k,k}^{it} \right| - \tilde{x}^{it}(k, u, v) \right|^2$$

The radar data is then updated in step **905** as:

$$\tilde{x}^{it}(k, u, v) = \tilde{x}^{it}(k, u, v) \left| \tilde{\alpha}_{k,k}^{it} \right|$$

This procedure loops for a finite number of iterations. Let the number of iterations be L. At the end of iterations, we obtain the following information: updated virtual array response (corrected for direction dependent phase which corrects for nodal displacement as well as amplitude/phase response per angle) $\tilde{x}(k, u, v)=\tilde{x}^{L}(k, u, v)$, an estimate of direction dependent amplitude correction,

$$|\tilde{\gamma}(u, v)| = \Pi_{it=1}^{L} \left| \tilde{\gamma}^{it}(u, v) \right|,$$

and an estimate of per channel amplitude variation

$$|\tilde{\alpha}_{k,k}| = \Pi_{it=1}^{L} \left| \tilde{\alpha}_{k,k}^{it} \right|.$$

The total per channel gain and phase correction terms are combined into a matrix, which is referred to as the diagonal antenna correction matrix. Using the exemplary mathematical model, this diagonal antenna correction matrix is defined as:

$$\tilde{A}_d^{-1} = \mathrm{diag}\left\{ |\tilde{\alpha}_{k,k}| e^{j \angle \tilde{\alpha}_{k,k}} \right\}, \quad 0 \le k \le N_{vrx} - 1$$

In an embodiment of the method and calibration system discussed herein, the ideal channel response can be refined to correct for setup error and nodal displacement error after the diagonal antenna correction. The MUSIC algorithm is used, which exploits knowledge of the number of objects to provide a super-resolution estimate of the actual object directions in each measurement. These directions are then used to recompute the ideal channel response. This refined ideal channel response is used during the cross-coupling calibration process.

FIG. **10** illustrates the calibration procedure for cross-coupling. First in step **1001**, a cross coupling estimate matrix is initialized to zeros. Then in step **1002**, a virtual channel is selected. In step **1003**, a list of retired cross channels is initialized to empty. Then in step **1004**, the measured response of the selected virtual channel is projected onto the ideal response for all cross channels. In step **1005**, the cross channel that corresponds to the maximum of the projection and is not yet retired is selected. The value of this projection is also recorded. In step **1006**, the contribution of the selected cross channel is removed from the measured response of the selected virtual channel. In step **1007**, if the contribution is greater than a given threshold, the cross-coupling matrix element corresponding to the selected virtual channel and the selected cross channel is set to the recorded projection value in step **1008**. Then in step **1009**, the selected cross channel is retired. The process repeats at the projection in step **1004**. If the contribution was not greater than a given threshold in step **1007**, then the process repeats at the virtual channel selection in step **1002** with the next virtual channel. This iterates until the process has completed for all virtual channels, as shown by step **1010**. In step **1011**, the cross-coupling matrix is then normalized by multiplying by the square root of the number of virtual antennas divided by the L2 norm squared of the diagonal elements of the cross-coupling matrix. The cross-coupling correction matrix is then estimated using the inverse of this cross-coupling matrix.

This cross-coupling calibration procedure can be described mathematically using the previous exemplary signal model. First in step **1001**, the cross-coupling matrix $\tilde{A}_c=0_{N_{vrx}-N_{vrx}}$. is initialized. Then the iterative procedure begins for each virtual channel. In step **1002**, the index of the current virtual channel is denoted as k. In step **1003**, initialize the list of retired cross channels S={ } is initialized. The projection of the k virtual channel response onto the ideal response for all cross channels in step **1004** is given by:

$$\beta_{k,m} = \sum_{u,v} \tilde{x}(k, u, v) y_{ideal}(m, u, v), \quad 0 \le m \le N_{vrx} - 1$$

Then in step **1005**, the channel, m_{max}, with the largest of $\beta_{k,m}$ is found as:

$$m_{max} = \underset{m \notin S}{\mathrm{argmax}} \left| \beta_{k,m} \right|$$

If this is the first iteration, $|\beta_{k,m_{max}}|$ is recorded as the largest coupling value, β_{max}. In this implementation of the algorithm, these values are used in the thresholding function in step **1007**. Then in step **1006**, the contribution to the measured channel response is removed from the selected cross-channel from above as:

$$\tilde{x}(k, u, v) = \tilde{x}(k, u, v) - y_{ideal}(m_{max}, u, v) \beta_{k,m_{max}}$$

In step **1007**, if the ratio between $|\beta_{k,m_{max}}|$ and β_{max} exceeds a certain threshold, Th_{cpl}, m_{max} is added to S in step **1009**, and $\tilde{A}_c(k, m_{max})$ is set to $\beta_{k,m_{max}}$ in step **1008**, and then the process goes to the projection in step **1004**. If the threshold test in step **1007** fails, the search for the k^{th} virtual channel is ended when the next virtual channel is repeated at step **1002**. Once the iterations are completed over all the virtual channels as indicated by step **1010**, the estimated cross-coupling matrix is normalized in step **1011** as follows:

$$\tilde{A}_c = \frac{\sqrt{N}}{\left\| \mathrm{diag}(\tilde{A}_c) \right\|_2^2} \tilde{A}_c$$

A final correction matrix is computed through matrix multiplication of the cross-coupling correction matrix and the diagonal antenna correction matrix. Using the previous

exemplary signal model, this correction matrix is defined mathematically as $\tilde{C}=A_c^{-1}\tilde{A}_d^{-1}$. This final correction matrix is implemented into the radar processing. The vector of data received at the virtual receivers is multiplied by this correction matrix before being multiplied by a steering matrix to achieve the calibrated beamformed output. The steering matrix is a stack of steering vectors, whose elements correspond to the desired complex beamforming weights. In the preferred embodiment, these vectors are the complex conjugate of the ideal channel response for the antenna array at a desired set of directions.

Thus, the exemplary embodiments discussed herein provide for the calibration of a radar system that corrects or adjusts for a misalignment between an array center of an antenna array of the radar system and a rotation center of the radar system via a platform of a calibration module that rotates the radar system in both azimuth and elevation. The calibration module calculates a misalignment between the array center of the antenna array and the rotation center of the radar system. At least one receiver of the radar system corrects for phase distortion and angle-of-arrival error due to the calculated misalignment. The misalignment between the array center of the antenna and the rotation center of the platform is a nodal displacement.

Changes and modifications in the specifically described embodiments can be carried out without departing from the principles of the present invention, which is intended to be limited only by the scope of the appended claims, as interpreted according to the principles of patent law including the doctrine of equivalents.

The invention claimed is:

1. A radar system comprising:

a transmitter communicatively coupled to a transmitter antenna array, wherein the transmitter is configured to transmit radio signals via the transmitter antenna array;

a receiver communicatively coupled to a receiver antenna array, wherein the receiver is configured to receive radio signals via the receiver antenna array that include radio signals transmitted by the transmitter and reflected from objects in an environment;

a calibration module comprising a platform configured to rotate the transmitter antenna array and the receiver antenna array in azimuth and/or elevation, wherein respective array centers of the transmitter antenna array and/or the receiver antenna array are not aligned with the platform's rotation center;

wherein the calibration module is configured to access receiver data from the receiver for each of a plurality of azimuth and/or elevation angles as the platform is rotated, wherein the calibration module is operable to calculate a misalignment value from the receiver data to define a misalignment between the array center of the receiver antenna array and the rotation center of the platform, and wherein the receiver is operable to perform antenna calibrations that includes accounting for the misalignment based upon the calculated misalignment value.

2. The radar system of claim **1**, wherein the platform is configured to rotate in discrete steps, and wherein the calibration module is operable to collect receiver data from the receiver at each discrete step.

3. The radar system of claim **2**, wherein the calibration module is configured to rotate the platform to discrete angles before collecting receiver data.

4. The radar system of claim **2**, wherein the platform is configured to rotate discretely for azimuth sweeps and/or elevation sweeps.

5. The radar system of claim **1**, wherein the platform is configured to rotate in a continuous sweep of angles, and wherein the calibration module is operable to collect receiver data while the platform is rotating.

6. The radar system of claim **5**, wherein the platform is configured to rotate continuously for azimuth sweeps and/or elevation sweeps.

7. The radar system of claim **1**, wherein the receiver is operable to perform the antenna calibrations to account for phase distortion and angle-of-arrival error.

8. The radar system of claim **1** further comprising a plurality of transmitters and a plurality of receivers, wherein each transmitter of the plurality of transmitters is communicatively coupled to the transmitter antenna array, and wherein each receiver of the plurality of receivers is communicatively coupled to the receiver antenna array.

9. The radar system of claim **8**, wherein the calibration module is configured to access receiver data from each receiver of the plurality of receivers for each of a plurality of azimuth and/or elevation angles as the platform is rotated, and wherein the calibration module is configured to calculate a respective misalignment value for each receiver of the plurality of receivers.

10. The radar system of claim **9**, wherein each receiver of the plurality of receivers is operable to perform antenna calibrations to account for the respective phase distortion and angle-of-arrival errors that includes accounting for the misalignment based upon the calculated misalignment values of each respective receiver of the plurality of receivers.

11. The radar system of claim **10**, wherein the misalignment between the array center of the receiver antenna array and the rotation center of the platform is a nodal displacement, and wherein the array center of the receiver antenna array is a nodal point.

12. The radar system of claim **11**, wherein the calibration module is operable to process phase distortion and angle-of-arrival error measurements into a correction matrix to calibrate for transmitter and/or receiver impairments which include at least one of phase error due to nodal displacement, per channel phase variation, direction dependent phase variation, per channel amplitude variation, direction dependent amplitude variation, and channel response cross-coupling.

13. The radar system of claim **12**, wherein the calibration module is operable to modify its measurement, collection, and calibration processing to optimize different objective functions including at least one of speed and manner of rotation, quantity of measurements collected, and the selection of antenna(s) and channel(s) transmitting and receiving the signals, and wherein these modifications also include parameters in the processing that controls the computation of the correction matrix and affect the processing speed and correction accuracy.

14. The radar system of claim **8** further comprising an antenna switch, wherein the transmitter antenna array and the receiver antenna array each comprise multiple antennas, and wherein each transmitter of the plurality of transmitters and each receiver of the plurality of receivers are coupled to the corresponding multiple transmitter antennas and multiple receiver antennas, respectively, via the antenna switch.

15. A radar system comprising:

a plurality of transmitters, each communicatively coupled to a transmitter antenna array, wherein each transmitter of the plurality of transmitters is configured to transmit radio signals via the transmitter antenna array;

a plurality of receivers, each communicatively coupled to a receiver antenna array, wherein each receiver of the

plurality of receivers is configured to receive radio signals via the receiver antenna array that include radio signals transmitted by the transmitters and reflected from objects in an environment;

a calibration module comprising a platform configured to rotate the transmitter antenna array and the receiver antenna array in azimuth and/or elevation, wherein respective array centers of the transmitter antenna array and the receiver antenna array are not aligned with the platform's rotation center;

wherein the calibration module is configured to access receiver data from each receiver of the plurality of receivers for each of a plurality of azimuth and/or elevation angles as the platform is rotated, wherein the calibration module is operable to calculate a respective misalignment value for each receiver of the plurality of receivers from the receiver data to define a misalignment between the array center of the receiver antenna array and the rotation center of the platform.

16. The radar system of claim **15**, wherein each receiver of the plurality of receivers is operable to perform antenna calibrations to account for respective phase distortion and angle-of-arrival errors that includes accounting for the misalignment based upon the calculated misalignment values of each respective receiver of the plurality of receivers.

17. The radar system of claim **16**, wherein the misalignment between the array center of the receiver antenna array and the rotation center of the platform is a nodal displacement, and wherein the array center of the receiver antenna array is a nodal point.

18. The radar system of claim **17**, wherein the calibration module is operable to process phase distortion and angle-of-arrival error measurements into a correction matrix to calibrate for transmitter and/or receiver impairments which include at least one of phase error due to nodal displacement, per channel phase variation, direction dependent phase variation, per channel amplitude variation, direction dependent amplitude variation, and channel response cross-coupling.

19. The radar system of claim **18**, wherein the calibration module is operable to modify its measurement, collection, and calibration processing to optimize different objective functions including at least one of speed and manner of rotation, quantity of measurements collected, and the selection of antenna(s) and channel(s) transmitting and receiving the signals, and wherein these modifications also include parameters in the processing that controls the computation of the correction matrix and affect the processing speed and correction accuracy.

20. A method for calibrating a radar system for system impairments, wherein the method comprises:

transmitting, with a transmitter, radio signals;

receiving, with a receiver, radio signals that include radio signals transmitted by the transmitter and reflected from objects in an environment;

wherein the transmitter and the receiver are coupled to an antenna array;

rotating, with a platform, the antenna array in both azimuth and elevation, and wherein an array center of the antenna array is not aligned with the platform's rotational center;

in the presence of at least one object, collecting from the receiver data defined by received radio signals reflected from the at least one object at selected azimuth and/or elevation angles, and calculating a misalignment value for a misalignment between the array center of the antenna array and the rotation center of the platform, and

correcting, with the receiver, antenna calibration errors that accounts for the misalignment based upon the misalignment value, wherein the misalignment between the array center of the antenna and the rotation center of the platform is a nodal displacement, and wherein the array center of the antenna array is a nodal point.

21. The method of claim **20**, wherein correcting for antenna calibration errors accounts for phase distortions and angle-of-arrival errors.

22. The method of claim **21** further comprising processing phase distortion and angle-of-arrival error measurements into a correction matrix to calibrate for transmitter and/or receiver impairments, which include at least one of phase error due to nodal displacement, per channel phase variation, direction dependent phase variation, per channel amplitude variation, direction dependent amplitude variation, and channel response cross-coupling.

23. The method of claim **22** further comprising solving phase error and amplitude variations via an iterative least squares optimization solution.

24. The method of claim **21** further comprising estimating, with the receiver, angles-of-arrival of the collected reflected signals or determining angles-of-arrival of the collected reflected signals based upon prior knowledge of the at least one object's location relative to the receiver.

25. The method of claim **21** further comprising modifying measurement, collection, and calibration processing to optimize different objective functions including at least one of speed and manner of rotation, quantity of measurements collected, and the selection of antenna(s) and channel(s) transmitting and receiving the signals, and wherein these modifications also include parameters in the processing that controls the computation of the correction matrix and affect the processing speed and correction accuracy.

26. The method of claim **20**, wherein the platform is rotated in either a continuous manner or in discrete steps, wherein, when rotating in discrete steps, the platform is rotated to discrete angles before collecting receiver data, and wherein, when rotating continuously, the platform is rotated in a continuous sweep of angles while collecting receiver data.

* * * * *